University College Cork, Ireland
Coláiste na hOllscoile Corcaigh

6

CO_2-Rich Melts in Earth

GREGORY M. YAXLEY, SUJOY GHOSH, EKATERINA S. KISEEVA, ANANYA MALLIK, CARL SPANDLER, ANDREW R. THOMSON, AND MICHAEL J. WALTER

6.1 Introduction

Carbonate-rich magmas in Earth play a critical role in Earth's deep carbon cycle. They have been emplaced into or erupted onto the crust as carbonatites (i.e. igneous rocks composed of >50% carbonate minerals, with SiO_2 contents <20 wt.%) for the last 2.5 Ga of geological history, and one volcano (Oldoinyo Lengai, Tanzania) has erupted sodic carbonatite lavas since 1960.[1]

Carbonate melts are inferred to exist in the upper mantle, largely on the basis of high-pressure experimental studies.[2–6] Their existence has also been inferred from the mineralogy and geochemistry of some suites of peridotite xenoliths recovered from alkali basalts,[7–9] and they have been observed directly in some inclusions in diamonds[10] and minerals in sheared garnet peridotite xenoliths.[11] They may also be present in the mantle transition zone or lower mantle in association with deeply subducted, carbonate-bearing slabs[12–14] and as inclusions in lower-mantle diamonds.[15]

Because of their low density, low viscosity, and ability to wet the surfaces of silicate minerals in the mantle,[16–18] carbonate melts are able to migrate upwards from their source regions rapidly and at extremely low melt fractions. They are able to transport significant amounts of incompatible trace and minor elements, volatile elements (H_2O, halogens, sulfur), and major components such as C, Mg, Ca, Fe, Na, and K. This renders them highly effective metasomatic agents and potentially major contributors to fluxes of carbon between reservoirs in the deep and shallow Earth. They are also of particular economic importance as hosts or sources of many critical metals, including the rare earth elements (REEs) Nb, Ta, P, and others.

In this chapter, we review the current understanding of the occurrence, stability, and role of carbonatites emplaced into or onto Earth's crust and carbonate melts in the deep Earth, from lower mantle to crust. We first outline constraints from high-pressure experimental petrology and thermodynamic considerations on their stability, as functions of variables such as pressure (P), temperature (T), and oxygen fugacity (fO_2). These constraints are then used in the context of different tectonic settings in Earth to infer the presence and nature of carbonate melts in those various locations.

Carbonate melts and carbonatite magmas are also often proposed to be genetically linked to some CO_2-bearing silicate melts (melts with >20 wt.% SiO_2 and dissolved, oxidized carbon, such as kimberlites, intraplate basalts, continental alkali basalts, etc.) through processes such as carbonate–silicate liquid immiscibility, crystal fractionation, and oxidation of diamond or graphite. Genetic relationships between carbonate melts and CO_2-bearing silicate melts in appropriate settings are also considered in this chapter.

6.2 Constraints on Carbonate Stability in Earth's Mantle

Critical to the stability, distribution, movement, and capacity for mass transport of carbonate melts at mantle pressure and temperature conditions is the fO_2 of the ambient mantle. This intensive variable exerts very strong control over the speciation of C in the mantle, which can range from highly reduced metal carbides, to methane fluids, to crystalline graphite or diamond, to oxidized carbon species such as CO, CO_2, or CO_3^{2-} in fluids or melts.[19]

The various species of carbon in the peridotite upper mantle are further limited by P–T–fO_2 conditions relative to: (1) the univariant graphite/diamond phase transition; (2) redox-dependent reactions such as enstatite–magnesite–olivine–diamond (EMOD) and enstatite–magnesite–forsterite–diopside–diamond (EMFDD; see below); (3) the carbonate peridotite (or eclogite) solidus; (4) decarbonation reactions involving carbonate minerals or carbonate in melts, and silicate phases, such as

$$\begin{array}{rcrcrcrcl} 4MgSiO_3 & + & CaMg(CO_3)_2 & = & 2Mg_2SiO_4 & + & CaMgSi_2O_6 & + & 2CO_2 \\ \text{orthopyroxene} & + & \text{dolomite} & = & \text{olivine} & + & \text{clinopyroxene} & + & CO_2 \end{array} \quad (6.1)$$

and (5) fluid absent equilibria such as

$$\begin{array}{rcrcrcl} 2MgSiO_3 & + & CaMg(CO_3)_2 & = & 2MgCO_3 & + & CaMgSi_2O_6 \\ \text{orthopyroxene} & + & \text{dolomite} & = & \text{magnesite} & + & \text{clinopyroxene} \end{array} \quad (6.2)$$

For example, the stability of carbonate phases versus diamond in a melt- or fluid-free, Ca-poor, magnesite harzburgite assemblage is limited in P–fO_2 space by the "EMOG/D" reaction (6.2) (enstatite–magnesite–olivine–graphite/diamond):[20,21]

$$\begin{array}{rcrcl} MgSiO_3 & + & MgCO_3 & = & Mg_2SiO_4 + C + O_2 \\ \text{orthopyroxene} & + & \text{magnesite} & = & \text{olivine} \end{array} \quad (6.3)$$

At depths from around 40–240 km on a typical cratonic geotherm, the univariant reaction will increase slightly in fO_2 from about –1.2 log units below fayalite–magnetite–quartz buffer (FMQ) to about –0.5 log units below FMQ.[21] At fO_2 values above this reaction, CO_2-fluid, dolomite, or magnesite will be stable depending on pressure relative to reactions (6.1) and (6.2). At fO_2 values below this reaction, graphite or diamond will be stable, depending on pressure relative to the univariant graphite–diamond reaction,[22] which lies at a pressure corresponding to about 150 km depth on a cratonic geotherm. The majority of kimberlite-borne garnet peridotite xenoliths for which fO_2 has been determined lie below EMOG/D, consistent with the sampling of diamond by deeply sourced kimberlites passing

through the cratonic lithosphere. This also means that carbonate melts are unlikely to be stable at depths throughout most of the cratonic mantle lithosphere, except in minor volumes (perhaps adjacent to conduits for kimberlites) where metasomatic enrichment processes may have locally oxidized the wall-rock significantly.[23]

In carbon-bearing lherzolite assemblages, the EMFDD reaction (6.4) limits carbonate stability in P–T–fO_2 space:

$$\begin{array}{l} 3MgSiO_3 \quad + CaCO_3 \quad = Mg_2SiO_4 + CaMgSi_2O_6 \quad + C + O_2 \\ \text{orthopyroxene} + \text{carbonate} = \text{olivine} \quad + \text{clinopyroxene} + \text{diamond/graphite} \end{array} \tag{6.4}$$

At 5 GPa, this reaction lies at about –1.2 log units at 500°C, decreasing to –1.5 log units at 1300°C, for realistic activities of the various components.[20]

Melting of carbon-bearing peridotite to form melts with high activities of carbonate therefore will be restricted to those regions of the peridotitic upper mantle where the oxidation state is consistent with carbonate stability (i.e. where fO_2 lies above the appropriate limiting reaction at given pressure and temperature).

The magnitude and variation of fO_2 in the mantle have been the subjects of many studies over recent decades. These have used measurements by a variety of techniques (wet chemical methods, Mössbauer spectroscopy, flank method, Fe K-edge micro-X-ray absorption near-edge structure spectroscopy) of $Fe^{3+}/\sum Fe$ in phases in peridotite xenoliths (spinel, garnet, pyroxenes) from the upper mantle, synchrotron Mössbauer measurements of Fe^{3+} in majoritic garnets from the sublithospheric upper mantle or mantle transition zone,[24] and $Fe^{3+}/\sum Fe$ measurements on primitive mid-ocean ridge basalt (MORB) glasses[25,26] coupled with high-pressure experimental and thermodynamic calibrations of relevant redox-controlling reactions.[27–29] These studies indicate that it is likely that carbonate stability in peridotite is generally limited to relatively shallow parts of the continental lithosphere (i.e. depths <~100 km; see Section 6.6.2 for more details). In the next section, we review high-pressure experimental constraints on the melting of carbonate peridotite.

6.3 Experimental Constraints on the Melting of Carbonate Peridotite in the Mantle

Many high-pressure experimental studies have investigated the phase and partial melting relations of (oxidized) carbonate-bearing mantle lithologies of peridotite at upper-mantle pressures.[3,5,6,30–41] The stable species of carbonate in the subsolidus peridotite upper mantle is controlled by some key carbonate–silicate reactions. These include reactions (6.1), (6.2), and (6.5):

$$\begin{array}{ccccccc} Mg_2SiO_4 & + & CO_2 & = & MgSiO_3 & + & MgCO_3 \\ \text{olivine} & + & CO_2 & = & \text{orthopyroxene} & + & \text{magnesite} \end{array} \tag{6.5}$$

These reactions have been delineated using high-pressure experiments in the CaO–MgO–SiO_2 ± H_2O (CMS ± H) system.[42–49]

In more complex natural systems, particularly those containing Fe and alkali metal components, reaction (6.4) intersects the peridotite + CO_2 system at the carbonate solidus at about 2.1 GPa and 1030°C (Hawaiian pyrolite + 5 wt.% dolomite[30]), dividing the shallow subsolidus lithospheric mantle into a shallower zone in which crystalline carbonate is unstable at the expense of CO_2 fluid and a deeper zone in which dolomite crystallizes as part of a spinel or garnet lherzolite assemblage. At the solidus, this reaction forms an approximately isobaric solidus ledge. At pressures greater than the ledge is a near-solidus field of sodic dolomitic carbonate melt in equilibrium with lherzolite residue. At pressures below the ledge, CO_2-rich fluid coexists with spinel lherzolite.

This reaction may act as a barrier to the migration of carbonate melts formed at higher pressures than reaction (6.1) to shallower depths in continental settings where geotherms are likely to intersect it. Dolomitic carbonate melts are predicted to react according to reaction (6.1), and this may lead to elimination of the melt and crystallization of secondary clinopyroxene and olivine at the expense of orthopyroxene and, in extreme cases, conversion of harzburgite or lherzolite mantle to orthopyroxene-free, clinopyroxene-rich wehrlite along with liberation of a CO_2-rich fluid. Such a process was inferred to have occurred in some spinel wehrlite xenoliths hosted in the Newer Volcanics of Victoria, southeastern Australia,[8,50] and in the Olmani Cinder cone, northern Tanzania.[51] It has been suggested that only in the circumstances where magma conduits become armored with orthopyroxene-free wehrlite are dolomitic carbonatites able to ascend to pressures less than the solidus ledge, potentially entering the crust, evolving to more calcic compositions, and, in some cases, becoming emplaced in the crust or erupted.[52]

In oceanic settings, convective geotherms are at higher temperatures than conductive geotherms in the continental lithosphere and are not expected to intersect the solidus ledge or by reaction (6.1). At higher pressures and temperatures (3.4 GPa, 1080°C),[30] the vapor-absent reaction (6.2) intersects the peridotite solidus, dividing the subsolidus regime into a lower-pressure field of dolomite garnet lherzolite and a higher pressure field of magnesite garnet lherzolite. Low-degree partial melts in experimentally investigated peridotite–$CO_2 \pm H_2O$ systems with natural compositions are generally broadly alkali rich and calcio-dolomitic to dolomitic in composition.[3] Solidus temperatures are considerably lower than those of volatile-free systems, and although experimental studies that include CO_2 *and* H_2O are relatively rare, the available evidence suggests solidus temperatures are even lower.[3,53]

In the following sections, we apply the experimental and other constraints to infer the existence and behavior of carbonate melts in different tectonic settings.

6.4 Carbonate Melts Associated with Subduction Zones

The mantle is believed to have played a key role in controlling the long-term carbon budget in the exosphere through cycling of carbon from the surface to the mantle and back again.[6,54,55] The deep carbon cycle is regulated at the surface by the quantity of carbon subducted into the mantle at convergent margins and by volcanic degassing of

mantle-derived melts releasing carbon into the exosphere at mid-ocean ridges, ocean islands, and arc volcanoes. A substantial proportion of the mass of carbon drawn into the mantle at subduction zones (anywhere between 20% and 100%) is recycled back to the surface via fore-arc degassing and arc magmatism,[56] as discussed in detail in Chapter 10 of this volume. Estimates of the net annual flux of carbon ingassing and outgassing via these processes are difficult to constrain with certainty, and range from negligible values to ~60 Mt/year net recycling.[6,56]

Carbon enters the mantle at subduction zones in sediments, altered oceanic crust, and mantle lithosphere, with the total input flux in the range of ~50–100 Mt/year at modern subduction zones.[6,56] Sedimentary carbon includes both biogenic organic carbon and carbonate. In more than a third of studied modern subduction zones, carbonate-rich materials make up a substantial fraction of the downgoing sediment, whereas in others it is absent altogether (e.g. Refs. 57, 58). However, organic carbon is expected to be at least a minor component in pelagic sediments and turbidites.[56]

Carbon is deposited during hydrothermal processes at mid-ocean ridges where carbonate (calcite and aragonite) forms during alteration of oceanic crust due to its reaction with CO_2 in seawater; biotic organic carbon in oceanic crust is minor relative to abiotic organic compounds and inorganic carbonates. The top few hundred meters of oceanic crust contain an average of ~2.5 wt.% CO_2, and at deeper levels the carbon content, mostly in the form of organic hydrocarbon species, drops below 0.2 wt.% throughout the remainder of the crustal section. Altered lithospheric mantle that is exposed to alteration by seawater also carries carbonate, although likely at an overall fraction that is much less than that of oceanic crust.[56,59]

Downgoing slab materials never reach temperatures high enough for "dry" partial melting during blueschist and eclogite facies metamorphism at fore-arc depths (up to ~80 km),[60] and portions of the slab that do not experience pervasive dehydration can effectively transport carbon to greater mantle depths. Nevertheless, at pressures above ~0.5 GPa, carbonate solubility in aqueous fluids increases with temperature,[61] so fluids produced by metamorphic devolatilization of the slab can be effective at dissolving carbonate minerals and mobilizing carbon.[62] Much of this carbon may be redistributed within the slab[63] or sequestered into serpentinized mantle rock that overlies the slab,[64–66] some of which in turn is dragged down with the descending slab.

At sub-arc depths (80–200 km), slab surface temperatures reach between 600 and 1000°C,[67] and carbonate mineral dissolution becomes much more efficient due to higher solubilities in hydrous fluids[68] and silicate melts[69] at these depths. In some cases, carbonatite liquids may also form via fluid-flux melting of carbonate-rich metasedimentary rocks[70] or carbonate-bearing metagabbros.[71] As a consequence, CO_2 ($\pm$ CO_3^{2-})-rich fluid phases migrating from the downgoing slab or from buoyantly upwelling slab diapirs[72,73] can introduce significant carbon flux from the slab to the overlying mantle wedge. Evidence in support of C-rich fluid phases at the slab surface comes from garnet and clinopyroxene inclusions in diamonds from Dachine, South America, which have major and trace element characteristics indicating growth at the surface of a subducting slab at ~200 km depth, possibly in metalliferous metasediment.[74]

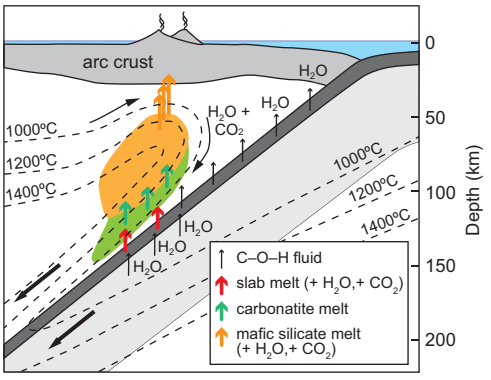

Figure 6.1 Schematic cross-section of a subduction zone (modified after Green[75]) depicting progressive slab devolatilization during subduction and zones of the mantle wedge containing carbonatitic and silicate-rich partial melts (green and orange fields, respectively).

Slab-derived fluids migrating into the overlying mantle will experience progressive heating as they ascend through the inverted temperature gradient of the mantle wedge (Figure 6.1).[75] The introduction of C–O–H fluids or melts results in a significant lowering of the wedge peridotite solidus, such that carbonatite liquids can be produced at temperatures below 950°C.[75] Such carbonatitic liquids (+ H_2O) are expected to be highly mobile, but will react with the wedge upon ascent and heating to produce carbonated hydrous silicate melts (>1020°C; Refs. 73, 75). Further ascent will favor further peridotite melting, increasing melt fractions, and diluting dissolved volatile contents. Upwelling from the hot core of the wedge may impart retrograde melt-rock or fluid-rock reactions, locking some carbonate (+ H_2O) phases in the mantle lithosphere and lower crust,[56] but the most volatile flux from the slab is expected ultimately to be delivered to the upper-arc crust via fractionating and degassing arc magmas.

The unique petrophysical evolution of magmas traversing the mantle wedge means that carbonatitic liquids are unable to be tapped from the mantle to the surface, which explains the lack of carbonatites found in supra-subduction zone settings.[76] Further, carbonated subarc mantle lithosphere and arc lower crust may eventually be preserved as subcontinental lithosphere through the reaction of volatile-rich melts with the mantle[77] or recycled into the convecting mantle, possibly thereafter to undergo melting to produce carbonatites in intraplate settings.

6.5 Melting of Subducted, Carbonated Sediment and Ocean Crust in the Deep Upper Mantle and Transition Zone

While subduction to ~200 km depth can remove a significant fraction of the initial downwelling carbon flux to the mantle wedge, experimental evidence of carbonate stability, modeling of phase equilibria, and slab devolatilization indicate that, in some subduction

zones, a substantial portion of subducted carbon or carbonate may make it past the dehydration zone and into the deeper mantle.[78,79] Experiments also suggest that carbonate may be reduced to elemental carbon (graphite or diamond) at depths shallower than 250 km in more reducing eclogitic assemblages, although for oxidation states typical of MORB (e.g. Ref. 80), eclogitic assemblages should remain in the carbonate stability field to at least 250 km.[28]

Inclusions of carbonate minerals in superdeep diamonds provide the strongest direct evidence for a carbonate component subducted past the volcanic front and at least to transition-zone depths.[81–84] In addition, the distinctive major and trace element compositions of silicate inclusions in many superdeep diamonds (e.g. majorite garnet, Ca- and Ti-rich perovskite) have been interpreted to preserve a direct record in their origin of a low-degree carbonated melt derived from subducted oceanic crust.[82,85,86] Both the carbon isotopic composition of the diamonds and the oxygen isotope composition of the inclusions provide further evidence for a key role of subducted crustal components in the origin of many superdeep diamonds and their inclusions.[87,88] Thus, it seems that melting of carbonated sediment and oceanic crust in the deep upper mantle and transition zone may play a key role in the deep carbon cycle.

Figure 6.2 compares the solidus determinations from published studies on the melting behavior of carbonated pelitic sediment and carbonated oceanic crust at upper-mantle and transition-zone conditions. The solidus of carbonated pelitic sediment was determined by Tsuno and Dasgupta[89] at 2.5–3.0 GPa and by Grassi and Schmidt[90] at 8–13 GPa, with melts ranging from granitic at low pressures to K-rich carbonatitic at higher pressures. On the basis of solidus determinations in these studies, only in the hottest subduction zones would melting of anhydrous carbonated sediments occur in the sub-arc region. The addition of water reduces the solidus of pelitic sediments, but unless sediments are water saturated, perhaps by fluxing of water-rich fluids from below, carbonated slab sediments may reach the deep upper mantle and transition zone.[91] At higher pressures approaching the transition zone, the experiments of Grassi and Schmidt[90] indicate that carbonated sediments can melt along warm and hot slab-top geotherms, but colder slabs could transport sedimentary carbonate into the deeper mantle (Figure 6.2).

There have been many experimental studies of melting carbonated basaltic compositions, both in simplified[92,93] and natural systems.[12,13,35,94–97] The small number of phases in basaltic compositions hampers studies in simplified compositions, whereas subtle compositional dependencies hamper studies in natural compositions. Indeed, subtle variations in bulk compositions between studies (Table 6.1) likely cause the significant variations in position and shape of the carbonated basalt solidus (e.g. Refs. 13, 98).

In the lower pressure range (e.g. <3–5 GPa), a carbonate phase is not always stable at the solidus depending on the bulk CO_2 and SiO_2 contents. In those with higher SiO_2/CO_2 ratios, CO_2 and/or silicate melts containing dissolved CO_2 define the solidus,[13,95,97] whereas compositions with lower SiO_2/CO_2 ratios showed carbonate stability and carbonate melt production along the solidus from low pressure.[13,35,98,99] Additionally, near-solidus melts have been identified with a wide range of compositions from mafic to

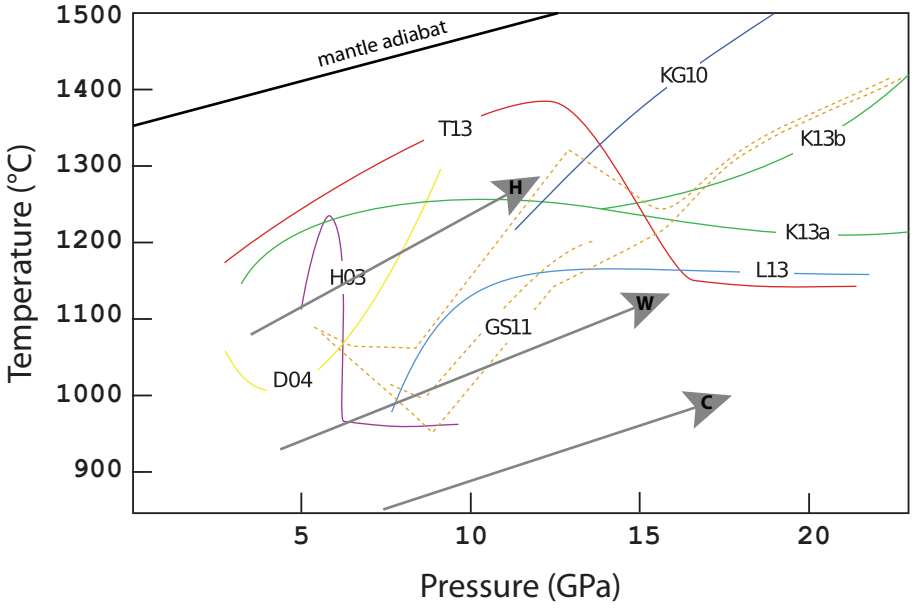

Figure 6.2 Summary of the experimentally determined solidus curves for carbonated pelitic sediment and basaltic compositions. Solidus curves for carbonated basalt are shown as solid colored curves and are from: Hammouda,[95] H03; Yaxley and Brey,[148] YB04; Dasgupta et al.,[94] D04; Keshav and Gudfinnsson,[186] KG10; Kiseeva et al.,[12] K13a,b; and Thomson et al.,[13] T13. Labels are keyed to the compositions listed in Table 6.1. Solidus curves for carbonated sediment are shown as dashed curves and are from: Tsuno and Dasgupta,[89] TD11; and Grassi and Schmidt,[187] GS11. Also shown is the solidus of alkaline carbonatite (Litasov et al.,[101] L13). The mantle adiabat is from Katsura et al.[188] Model geotherms at the top of a subducting slab are extrapolations shown for examples of hot, warm, and cold slabs.[67]

silicic. In some cases silicate melts are observed at the solidus before carbonate melts, whereas in other cases this relationship is reversed, and both kinds of melts have been interpreted to coexist together as immiscible liquids.[12,99,100] The observation of immiscible melts may reflect the maximum CO_2 solubility in silicate melts, and the appearance of liquid immiscibility will therefore depend on the CO_2 content of the bulk composition.

At higher pressures of the deep upper mantle and transition zone, starting compositions again show remarkable control of melting behavior (Figure 6.2). When comparing the carbonated starting compositions used in the various studies, there are considerable differences, perhaps most notably in SiO_2 and CO_2 contents and Ca#. Thomson et al.[13] observed that the Ca# has an important controlling effect on the stable carbonate phase at the solidus beyond the pressure of dolomite breakdown (>~10 GPa). Phase relations apparently preclude coexistence of magnesite and aragonite in majorite- and clinopyroxene-bearing assemblages, and which of these carbonate phases is stable has an important controlling effect on the solidus shape and melt compositions.

Table 6.1 *Bulk compositions (as wt.%) of anhydrous MORB and carbonated MORB used in melting studies*

MORB examples[a]	G12 All MORB	Y94 MAN-7	W99 JB1	H03 OTBC[b]	D04 SLEC1	K13a GA1cc	K13b Volgacc	T16 ATCM1
SiO_2	50.47	47.71	53.53	47.23	41.21	45.32	42.22	50.35
TiO_2	1.68	1.71	1.44	–	2.16	1.34	1.43	1.33
Al_2O_3	14.7	15.68	14.85	15.35	10.89	14.88	15.91	13.66
FeO	10.43	9.36	7.92	8.93	12.83	8.85	9.46	11.35
MnO	0.18	0.18	0.16	–	0.12	0.15	0.14	0.21
MgO	7.58	8.43	7.64	6.24	12.87	7.15	7.64	7.15
CaO	11.39	11.73	9.12	14.77	13.09	14.24	14.85	10.8
Na_2O	2.79	2.76	2.64	2.91	1.63	3.14	3.36	2.48
K_2O	0.16	0.23	1.31	0.02	0.11	0.4	0.42	0.06
P_2O_5	0.18	0.02	–	–	–	0.14	0.15	0.1
CO_2	–	–	–	4.43	5.0	4.4	4.4	2.52
Total	99.57	99.81	98.61	99.98	99.91	100.01	99.98	100
Ca#[c]	0.38	0.38	0.38	0.48	0.32	0.46	0.45	0.36
Mg#[c]	0.57	0.62	0.62	0.56	0.64	0.59	0.59	0.53

[a] G12 = Gale et al.;[190] Y94 = Yasuda et al.;[191] W99 = Wang and Takahashi;[192] D04 = Dasgupta et al.;[94] H03 = Hammouda;[95] K13 = Kiseeva et al.[12]

[b] OTBC additionally contains 1200 ppm H_2O.

[c] Ca number = Ca/(Ca + Mg + Fe); Mg number = Mg/(Mg + Fe).

In Ca-rich carbonated basalt bulk compositions, the stable phase is aragonite, which is also a host for sodium.[12] However, in lower Ca# bulk compositions, magnesite is stable, and because sodium is relatively insoluble in magnesite, another Na-rich carbonate stabilizes in the subsolidus assemblage at pressures greater than ~15 GPa. The appearance of a Na-carbonate phase in the subsolidus produces a dramatic lowering of the melting temperature and a deep trough along the solidus between ~10 and 15 GPa that is not observed where aragonite is stable (Figure 6.2). When Na-carbonate occurs on the solidus, it is observed that the melting temperature at pressures >~15 GPa (~1150°C) is indistinguishable from that observed for a simplified Na-carbonate-rich bulk composition at these conditions (Figure 6.2).[101] As the majority of natural MORB compositions, fresh and altered, fall to the Mg-rich side of the majorite–clinopyroxene join, they should have magnesite and not aragonite as the stable carbonate at high pressures and experience the lowered solidus at transition-zone conditions.[13]

Figure 6.3 shows melt compositions projected onto a plane differentiating major and minor components of sediment and basalt-derived carbonated melts, demonstrating a generally continuous evolution with increasing pressure and temperature. The lowest-degree melts of carbonated basalt are highly calcic, even when the subsolidus carbonate is magnesite, because magnesite is the liquidus phase in most carbonate systems.[101] Carbonated melts are enriched in

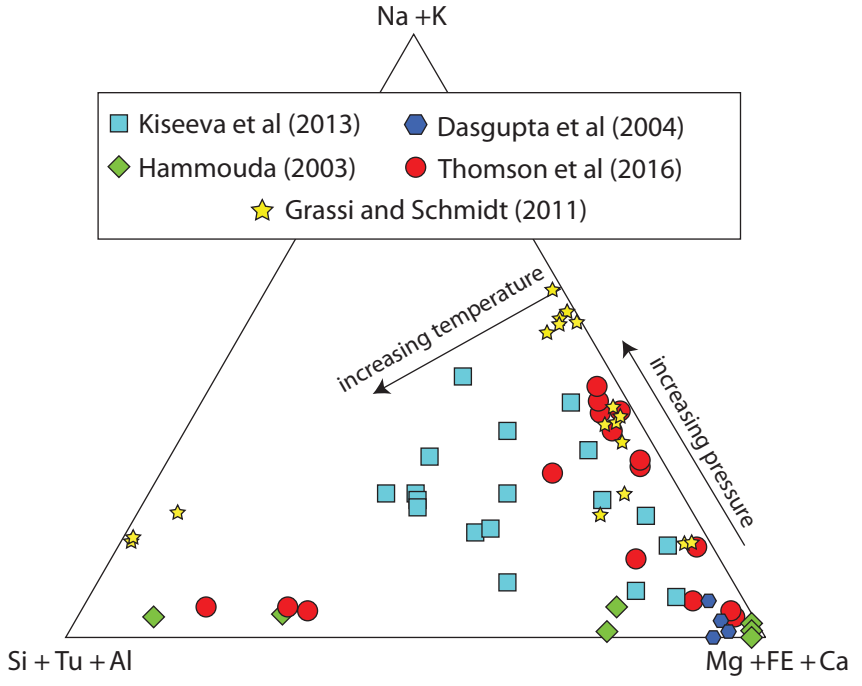

Figure 6.3 The compositions of partial melts from carbonated natural basalt and sediment from the studies of Hammouda,[95] Dasgupta et al.,[94] Kiseeva et al.,[12] Thomson et al.,[13] and Grassi and Schmidt.[90] The generalized effects of increasing pressure and temperature are also shown.

incompatible elements and have high concentrations of TiO_2, P_2O_5, and alkalis (Na_2O and K_2O), the relative abundances of which will be controlled by the bulk composition of the protolith. Sediment melts are dominated by potassium, whereas melts from carbonated basalt have alkali contents that are dominated by Na_2O. Melt Na_2O content increases systematically with pressure in basaltic compositions, resulting from the decreasing compatibility of Na_2O in the coexisting residual phase assemblage. Thomson et al.[13] observed that melt compositions of carbonated basalt in the transition zone remain approximately constant over a wide temperature interval of >300°C above the solidus, and only when temperature exceeds ~1,500°C does the silica content of the melt increase. This behavior is reminiscent of the melting behavior observed in carbonated peridotite assemblages at lower pressures.[102]

6.6 Carbonate Melts and Kimberlites in the Cratonic Lithospheric Mantle

The cratonic mantle lithosphere underlies ancient, continental blocks that have been geologically stable for billions of years. It is chemically depleted, thick, and buoyant. Unlike other tectonic settings, any surface expression of cratonic magmatism is manifested by emplacement of small-volume, rare, exotic, volatile-rich, alkali- and carbonate-rich magmas, such as carbonatites, kimberlites, lamproites, various lamprophyres, and other

highly silica-undersaturated magmas,[103,104] all of which have a deep mantle origin. Describing the detailed petrology of these rocks is beyond the scope of this chapter, and the reader is referred to the work of Jones et al.[76] Below, we give a short overview of an important carbonate-bearing silicate volcanic rock found in cratonic settings: kimberlites.

6.6.1 Kimberlites

Kimberlites are volatile (chiefly CO_2)-rich, silica-poor alkaline, ultrabasic magmas generally believed to be derived from a depth of $\geq$150–250 km and almost exclusively emplaced into cratonic crust. Kimberlite magmas are economically significant because of their association with diamonds. They have been subdivided into two major groups on the basis of petrographic and geochemical characteristics: Group 1 kimberlites and Group 2 kimberlites.[105–107] Group 1 kimberlites are CO_2-rich, potassic, ultrabasic rocks with a typical porphyritic texture, with large phenocrysts of most commonly olivine surrounded by a fine-grained matrix consisting of olivine, phlogopite, spinel, ilmenite, monticellite, calcite, apatite, perovskite, and other phases.[108] Group 2 kimberlites, or orangeites, are restricted to southern Africa. However, similar rocks have also been identified in Australia, India, Russia, and Finland. They are texturally similar to the Group 1 kimberlites, but have distinct compositional and isotopic differences, manifested mainly by the presence of phlogopite, K–Ba–V titanites, and Zr-bearing minerals, such as kimzeytic garnets,[108] lower ε_{Hf} and ε_{Nd} values, and high radiogenic ^{87}Sr isotope compositions.[109]

Similar to carbonatites, kimberlites are volumetrically very minor, but they are widespread throughout the cratonic parts of continents, with the latest discoveries extending the Gondwanan Cretaceous kimberlite province to Antarctica.[110] The main difference with carbonatites is in their origin in the subcratonic lithospheric or asthenospheric mantle enriched by an ocean island basalt source in the case of Group 1 kimberlites, whereas Group 2 kimberlites are derived from metasomatized lithospheric mantle,[107,111] and their eruption is predominantly through stable parts of cratons.[112] To our knowledge, there are no reported occurrences of kimberlites in the oceanic crust.[112,113]

The accurate determination of the kimberlite parental magma composition and its origin is hampered by the ubiquitous presence of a large fraction of foreign materials (mantle and crustal xenocrysts and xenoliths), in particular olivine crystals, collected from lithospheric mantle during their ascent to the surface, and by low-temperature alteration during and after emplacement. Petrological studies of the unaltered Udachnaya kimberlite pipe in the Siberian Craton showed high enrichment in CO_2, halogens, and alkalis, resulting in a hypothesis in which genetic links between kimberlites and carbonatites were important.[114,115] Later, experimental studies concluded that magmas potentially parental to kimberlites originate as dolomitic carbonate liquids in metasomatized, oxidized zones in the deep cratonic lithospheric mantle[23] that segregate and become progressively more silicate-rich due to the assimilation of silicate material (mostly orthopyroxene) during ascent through the refractory lithosphere.[116]

Alternative models are based on high-pressure experimental studies of estimated compositions of melts parental to kimberlites and have attempted to identify pressure, temperature, and volatile conditions at which the melts are multiply saturated in garnet peridotite phases.[117,118] Such studies have indicated that the most likely source for kimberlite parental melts is hydrous, carbonate-bearing garnet harzburgite in the deep cratonic lithospheric mantle or sublithospheric asthenosphere.

In either case, kimberlite genesis clearly requires a sufficiently oxidized mantle for crystalline carbonate (Ca-magnesite) to be stable in the peridotitic source,[23] and the source is constrained to be greater than ~150 km depth in the cratonic lithospheric mantle because of the presence of xenocrystic diamonds.

6.6.2 Redox Constraints on Carbonate Stability in the Cratonic Lithospheric Mantle

In any volume of the cratonic mantle, in the absence of externally derived melts or fluids, the local fO_2 is controlled by silicate or oxide mineral exchange equilibria such as reactions (6.6)–(6.9), which involve oxidation of Fe^{2+}-bearing components and reduction of Fe^{3+}-bearing components.

$$\underset{\text{orthopyroxene}}{6FeSiO_3} + \underset{\text{spinel}}{2Fe_3O_4} = \underset{\text{olivine}}{6Fe_2SiO_4} + O_2 \tag{6.6}$$

$$\underset{\text{spinel}}{2Fe_3O_4} + \underset{\text{orthopyroxene/olivine}}{3SiO_2} = \underset{\text{olivine}}{3Fe_2SiO_4} + O_2 \tag{6.7}$$

$$\underset{\text{garnet}}{2Fe^{2+}{}_3Fe^{3+}{}_2Si_3O_{12}} = \underset{\text{olivine}}{4Fe_2SiO_4} + \underset{\text{orthopyroxene}}{2FeSiO_3} + O_2 \tag{6.8}$$

$$\underset{\text{garnet}}{2Ca_3Fe_2Si_3O_{12}} + \underset{\text{garnet}}{2Mg_3Al_2Si_3O_{12}} + \underset{\text{orthopyroxene}}{4FeSiO_3} = \underset{\text{garnet}}{2Ca_3Al_2Si_3O_{12}} + \underset{\text{olivine}}{4Fe_2SiO_4} + \underset{\text{opx}}{6MgSiO_3} + O_2 \tag{6.9}$$

For example, (6.6)–(6.9) have been calibrated experimentally,[21,27,119–121] meaning that, in principle, the fO_2 of a spinel or garnet peridotite from the upper mantle can be determined if the activities of the Fe-bearing components in the minerals that contain Fe^{2+} and Fe^{3+} can be determined, along with other mineral component activities, pressure, and temperature.

These experimental calibrations can be combined with conventional thermobarometry to calculate the variation in fO_2 as a function of depth in the peridotite lithospheric upper mantle, as recorded by peridotite xenoliths from kimberlites in the case of cratonic mantle lithosphere, for example. The uppermost cratonic mantle lithosphere based on spinel peridotite xenoliths sampled by kimberlites has fO_2 between 0 and –1 log units relative to FMQ

for primitive ($\Delta \log fO_2^{FMQ}$),[122] well within the carbonate stability field. In the garnet peridotite facies, fO_2 decreases systematically with increasing pressure (depth) through the cratonic lithosphere (Figure 6.4),[23,122,123] although the xenolith record exhibits complications associated with oxidative overprinting associated with metasomatism, particularly at depths >150 km. Decreasing fO_2 with increasing depth is expected on a thermodynamic basis, because of the molar volume changes of reactions such as (6.8) and (6.9).[27,124] It is therefore likely that melts with high carbonate activities are unstable relative to graphite or diamond at depths greater than ~90–120 km in the cratonic lithospheric mantle.

At depths of ~250–300 km, the fO_2–P path is expected intersect the Ni precipitation curve, an FeNi alloy will exsolve from peridotite, and fO_2 will be buffered near the iron–wüstite (IW) buffer deeper into the upper mantle. In the presence of metallic FeNi alloy, some reduced carbon will be accommodated as (Fe,Ni) carbides. Rohrbach et al.[125] have

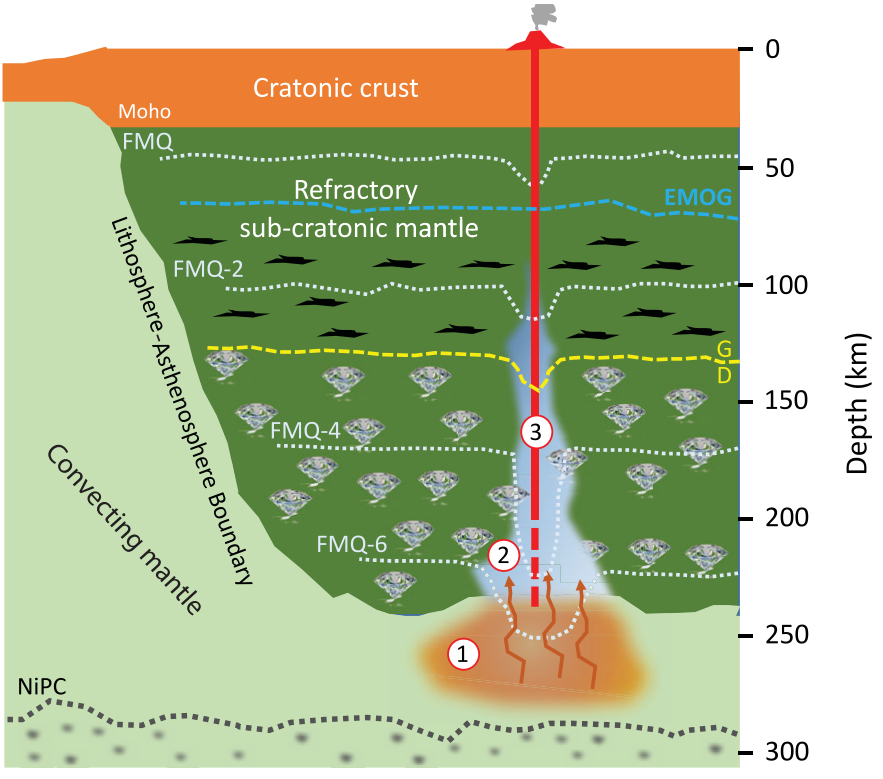

Figure 6.4 Highly schematic representation of a section through Earth's upper mantle modified from figure 2c of Foley and Fischer,[112] showing fO_2 as a function of depth. The dashed white contours are approximate contours of fO_2 variation in the cratonic lithosphere based on studies of garnet peridotite xenoliths (references in the text). The dashed yellow line is the graphite–diamond transition for a typical cratonic geotherm (38 mW m^{-2}). The red line (3) represents the path of an erupting kimberlite and the blue zone (2) near the base of the lithosphere represents a local mantle volume metasomatized to higher fO_2 by asthenospheric melts derived from the brown field labeled (1).

calculated that, assuming the mantle contains 50–700 ppm FeNi and 50–500 ppm C at 300 km depth, it would contain an assemblage of $(Fe,Ni)_3C$ + FeNi alloy + diamond or an Fe–Ni–S–C melt.[126]

Although the cratonic mantle becomes more reduced with increasing depth, local redox heterogeneities may be introduced, particularly at depths greater than 150 km, by metasomatic fluids such as carbonate-bearing silicate melts[23,127] with low carbonate activities,[21] possibly derived from the asthenosphere or from oxidized crustal material recycled via subduction. In some cases, the degree of oxidation in the lower part of the cratonic lithospheric upper mantle could be sufficient to stabilize crystallization of carbonates (magnesite in peridotite), which, in the presence of H_2O, could melt and produce magmas parental to kimberlites.[117,118]

6.6.3 The Involvement of Carbonate Melts in Metasomatism of the Deep Cratonic Lithospheric Mantle

Apart from carbonatites and kimberlites that were emplaced into or erupted onto the crust, CO_2-rich fluids, carbonate melts, or carbonated silicate melts are often inferred to be major agents of mantle metasomatism and trace element enrichment in the lithospheric mantle. Unlike, for example, alpine massifs, most peridotite and eclogite xenoliths carried to the surface by kimberlites are chemically enriched relative to the depleted lithospheric mantle. It may be that the degree of this enrichment was previously severely underestimated[112,128] and that CO_2-rich metasomatism is a widespread process throughout the cratonic mantle.

It is not always easy to distinguish and characterize the exact nature of a particular metasomatic overprint observed in natural rocks. Given the giga-year ages of the cratonic lithospheric mantle, there is a likelihood of multiple melting (i.e. depletion) and subsequent re-enrichment events. Moreover, the challenge of deciphering a particular metasomatic event in a given mantle xenolith is exacerbated by the possibility of multiple types of percolating fluids. For instance, in addition to the carbonatitic CO_2-rich metasomatism, an H_2O-rich alkali silicate metasomatism, perhaps of a proto-lamproite type, has been reported.[129–131]

At the reduced conditions likely to exist in much of the deep cratonic lithospheric mantle and underlying asthenosphere, carbonate phases are not expected to be generally stable and so melts with high carbonate activities such as carbonatites will likely not form, except locally in localized zones already strongly oxidized due to earlier metasomatism.[23] Carbon transport will likely be as low activity carbonate dissolved in undersaturated silicate melts[21] or as CH_4 + H_2O fluids.[128,132,133] However, it should also be noted that the depth–fO_2 profile of the asthenospheric mantle is not necessarily the same as that observed in xenolith studies from the cratonic mantle or inferred from thermodynamic calculations. Based on CO_2–Ba–Nb systematics of oceanic basalts, the convecting mantle may in fact be considerably more oxidized at pressures greater than about 3 GPa.[134]

If undersaturated silicate melts with dissolved carbonate or CO_2 at low activities form as a result of adiabatic upwelling in plumes or rifts, segregate from their asthenospheric

sources, and percolate upwards into parts of the cooler, deep cratonic lithosphere, they will freeze into the lithospheric mantle as the appropriate peridotite + volatile solidus is locally crossed. Oxidized carbon species will be exsolved from the melt during crystallization and would reduce to C or CH_4 ($CO_2 = C + O_2$; $CO_2 + 2H_2O = CH_4 + 2O_2$) because of the low ambient fO_2 in the deep cratonic lithosphere. Fe^{2+} in the melt and the wall rock will oxidize to Fe^{3+} ($2FeO + ½O_2 = Fe_2O_3$) and be incorporated into garnet and pyroxenes, leading to the observed increase in lithospheric fO_2 associated with metasomatism. The increased activity of H_2O may cause a decrease in the solidus temperatures of peridotite locally and lead to partial melting in a process known as hydrous redox melting. Only after sufficient oxidation by this type of metasomatic process could the fO_2 of the deep cratonic lithospheric mantle be raised sufficiently to allow carbonate stability and the formation of carbonatites, kimberlites, and related rocks at these depths.

6.7 Carbonate Melts beneath Ocean Islands in Intraplate Settings

Observations from natural samples indicate the role of CO_2, specifically CO_2-rich silicate melts, in the metasomatism of the upper mantle beneath ocean islands in intraplate settings. Carbonate phases, interpreted to be quenched carbonate liquids, have been identified in metasomatized harzburgite xenoliths in the Kerguelen and Canary Islands.[135,136] These carbonate inclusions are texturally associated with silicate glass inclusions, either as globules within a silicate matrix or as intimate associations with silicate inclusions. Such textural associations between the carbonate-rich phases and the silicate glasses have led to the conclusion that the carbonate-rich phases are products of immiscibility of a single carbonated silicate melt phase that exists at depth, possibly at upper-mantle conditions. Geochemical modeling of rejuvenated Hawaiian lavas also indicates the presence of carbonate-rich liquids in the source of these lavas.[137]

6.7.1 How Do CO_2-Rich Silicate Melts Form in the Upper Mantle? Can These CO_2-Rich Melts Explain the Chemistry of Erupted Magmas in Intraplate Ocean Islands?

Previous experimental studies have demonstrated that CO_2-rich silicate melts can be produced in upper-mantle conditions by the following mechanism. Carbon may exist in its oxidized form as carbonate mineral or as liquid in the mantle at fO_2 values that are about 2 log units higher than that of the IW buffer (given by equilibrium (6.10)):

$$\underset{\text{iron}}{2Fe} + O_2 \quad = \quad \underset{\text{wüstite}}{2FeO} \tag{6.10}$$

which corresponds to depths above 150–250 km[21,138] in the oceanic lithosphere. Carbonate may be present deeper in the mantle in locally oxidized regions.[139,140] Due to cryoscopic depression of the freezing point, carbonate-bearing lithologies (peridotite and recycled

oceanic crust or eclogite) have lower solidus temperatures than nominally anhydrous or carbonate-free lithologies, as demonstrated by experimental studies.[5,33,47,94–96,99,141–148] This implies that in an upwelling mantle partial melting of carbonated lithologies is initiated deeper than in the surrounding carbonate-free lithologies. Near-solidus partial melting of carbonated peridotite and/or carbonated recycled oceanic crust (eclogite) produces carbonatitic liquids (>25 wt.% CO_2, <20 wt.% SiO_2). These carbonatitic liquids tend to be very mobile owing to their low viscosities and low dihedral angles,[149] which lead to their escape from the site of generation. These rising liquids can cause flux-based partial melting of peridotite and eclogite in an adiabatically upwelling plume mantle in intraplate settings, which produces CO_2-bearing silicate melts (Figure 6.5a).

Peridotite is the dominant lithology of Earth's mantle. This increases the likelihood of partial melts of CO_2-bearing peridotite being the best candidates for explaining the geochemistry of ocean island basalts that commonly erupt in ocean islands in intraplate settings. The next likely candidate for ocean island basalts would be partial melts of CO_2-bearing eclogite, given recycled oceanic crust forms the dominant chemical heterogeneity in Earth's mantle.[150] Comparisons of the major element chemistry of partial melts of CO_2-bearing peridotite and eclogite with natural, near-primary ocean island basalts indicate that carbonated peridotite-derived partial melts are too TiO_2 poor,[151] while carbonated eclogite-derived partial melts are too depleted in MgO.[99] Also, the peridotite-derived partial melts can explain the MgO content very well for the ocean island basalts, while the eclogite-derived partial melts can explain the TiO_2 contents. This implies that the source of ocean island basalts would be best explained by a hybrid source involving contributions from both peridotite (high MgO) and eclogite (high TiO_2). A previous study indicated a couple of geodynamic scenarios involving CO_2-bearing eclogite and peridotite as the source of ocean island basalts (Figure 6.5b).[152]

Deep carbonatites are formed by very-low-degree partial melting of carbonate-bearing eclogites that are present in deep, locally oxidized upper-mantle domains. These carbonatites rise up and cause flux melting of overlying volatile-free eclogites. The flux melting produces eclogite-derived carbonated silicate melts (ranging from basanites to andesites) that are out of chemical equilibrium with their surrounding peridotite and undergo reactive infiltration. The metasomatic process or melt-rock reaction associated with such reactive infiltration forms ocean island basalts.

Deep carbonatites can also be generated by very-low-degree partial melting of graphite/diamond-bearing peridotite or eclogite at the redox front (150–250 km depth, where reduced carbon in the form of diamond/graphite is oxidized to a carbonatitic melt). These carbonatites can cause fluxed melting of volatile-free eclogite and can undergo subsequent reactive infiltration through the peridotite, as described above.

A question arises as to whether the involvement of CO_2 in the source is required for all ocean island basalts. Studies have shown that basanitic ocean island basalts can be explained by partial melting of volatile-free peridotite ± eclogite in the source; however, more silica-undersaturated ocean island basalts such as nephelinites and melilitites require the involvement of CO_2.[152,153]

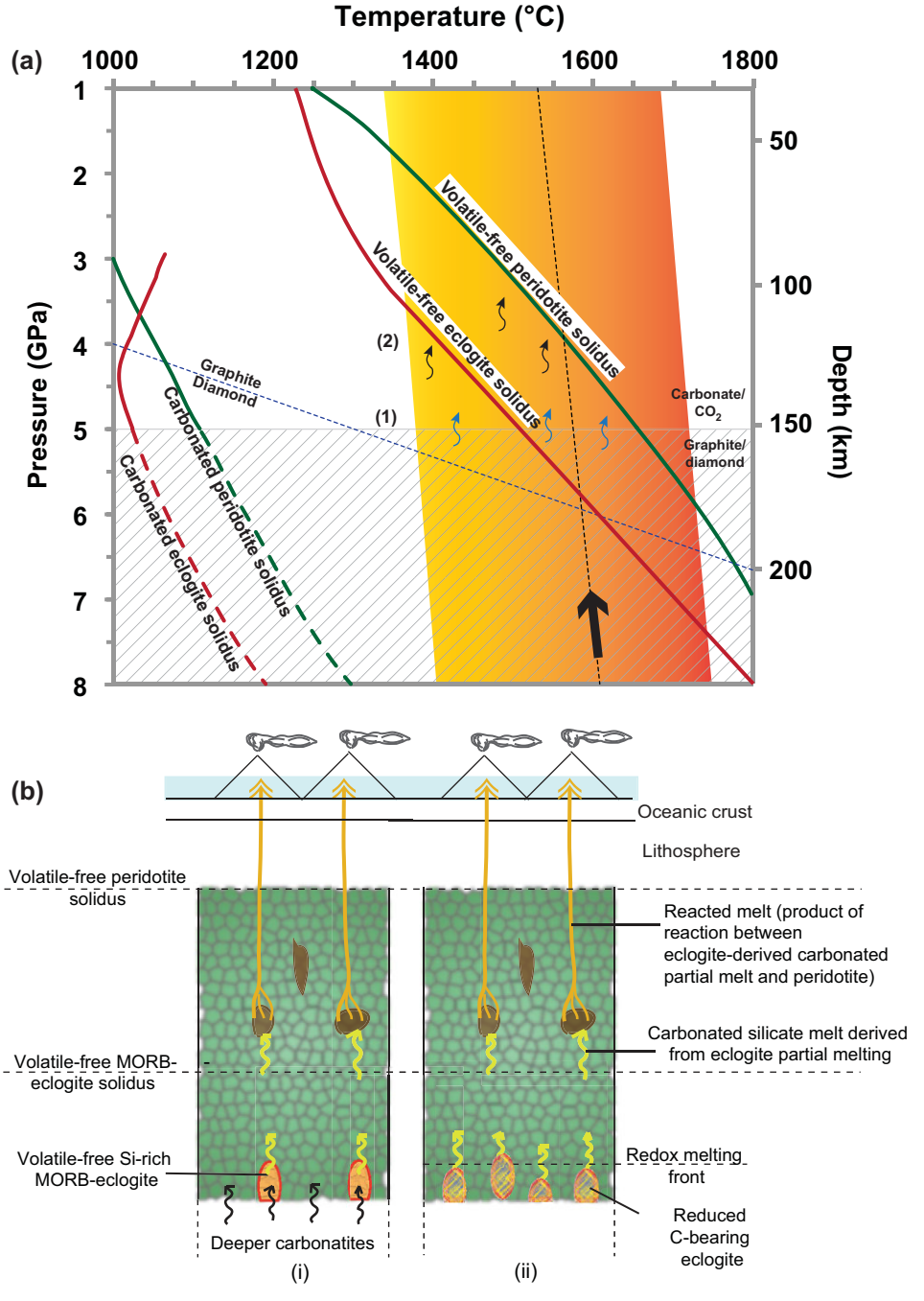

Figure 6.5 (a) Pressure–temperature plot showing the generation of carbonated silicate melt in Earth's upper mantle. A parcel of carbon-bearing mantle peridotite with pods of eclogite upwells

6.7.2 Effect of CO_2 on the Reaction between Eclogite-Derived Partial Melts and Peridotite

CO_2 dissolves in silicate melts as both molecular CO_2 and CO_3^{2-} anions. When network-modifying cations (those that depolymerize the silicate network) such as Na^+, K^+, Ca^{2+}, Mg^{2+}, and Fe^{2+} are available in the silicate melt, CO_3^{2-} bonds with these cations.[154] These carbonate complexes result in the cations being removed from their network-modifying roles. Thus, these carbonate complexes give rise to pockets of polymerized networks in the silicate melt structure.[155]

When eclogite-derived melts react with olivine- and orthopyroxene-bearing peridotite, the following equilibrium (6.11) buffers the thermodynamic activity of SiO_2 (a_{SiO2}) in the reacted melt:

$$\underset{\text{olivine}}{Mg_2SiO_4} + \underset{\text{melt}}{SiO_2} = \underset{\text{orthopyroxene}}{Mg_2Si_2O_6} \quad (6.11)$$

The localized separation of polymerized silicate networks and carbonate complexes in the silicate melt structure results in the requirement for excess free energy of mixing between the two structural components. This increases the activity coefficient of SiO_2 in the melt (γ_{SiO2}). Higher γ_{SiO2} when a_{SiO2} is buffered results in a decrease in the mole fraction of SiO_2 (X_{SiO2}) in the melt.[151] Thus, involvement of CO_2 in the melt-rock reaction decreases the SiO_2 content of the product melt, driving eclogite-derived basanites and andesites to produce nephelinites and melilitites (depending on the amount of CO_2 available in the system).[152,153]

Figure 6.5 (*cont.*) beneath ocean islands along an adiabat (bold arrow along the dotted line). As it upwells, redox melting takes place when the mantle crosses over from the stippled zone where the carbon is present in reduced form (either as graphite or as diamond[21,138]) to the overlying zone where carbon is present in its oxidized form (as carbonates or as CO_2 vapor at pressures lower than 2 GPa[3]). At the redox front, reduced carbon present in the eclogite or peridotite oxidizes to form trace to minor amounts of carbonatitic melt (labeled (1)). The carbonatitic melt causes fluxed partial melting of eclogite and peridotite because the carbonated solidi of peridotite and eclogite are at much lower temperatures at the pressure range of the upwelled parcel of mantle (labeled (2)). The fluxed partial melting of eclogite and peridotite produces carbonated silicate melts in the upper mantle. The volatile-free solidi of peridotite[189] and eclogite,[191] the carbonated solidi of peridotite[33,142] and eclogite,[148] the graphite–diamond transition,[193] and the range of mantle potential temperatures in Earth's upper mantle (orange shaded area) from ridges[194] to plumes[195] are plotted for reference. The broken curves for carbonated solidi are only applicable for locally oxidized domains in the mantle where carbonates can exist at depths below the redox-melting front. (b) Geodynamic scenarios involving carbonated eclogite and peridotite in the source of ocean island volcanism in intraplate settings (modified from a previous study[152]). (i) This scenario is applicable for locally oxidized domains in the mantle where deeper carbonatites generated by very-low-degree partial melting of carbonated peridotite and/or eclogite rise upwards and cause fluxed partial melting of volatile-free eclogite at shallower depths in the upper mantle. The carbonated partial melt of eclogite, a basanite, or andesite (a lower eclogite to carbonate ratio produces basanite, while a higher ratio produces andesite) reacts with subsolidus volatile-free peridotite. The melt-rock reaction produces product melts that display similarity in composition with ocean island basalts. (ii) Reduced carbon-bearing eclogite upwells and produces carbonated silicate partial melts of eclogite after crossing the redox-melting front. The carbonated silicate partial melt of eclogite reacts with the surrounding subsolidus volatile-free peridotite, and a similar melt-rock reaction as proposed in (i) takes place.

A higher γ_{SiO2} and an increased degree of polymerization of the silicate domain of the melt network also imply that saturation of orthopyroxene is preferred over saturation of olivine in the residue of melt-rock reaction. Thus, the stability field of orthopyroxene is enhanced over that of olivine.[47,151–153] Also, cations such as Ca^{2+}, Mg^{2+}, Na^{+}, and K^{+} prefer to enter the melt structure to form carbonate complexes in the presence of CO_2. This enhances the calcium, magnesium, and alkali contents of the product melts.

6.8 Carbonate Melts under Mid-ocean Ridges

Along mid-ocean ridges, where divergent tectonic plates move apart from each other, the rising asthenospheric mantle decompresses and partially melts to create basaltic magma that buoyantly rises to Earth's surface and solidifies to form new oceanic crust. During decompression melting, volatile-free mantle lithologies melt at ~60 km, producing silicate melts.[156] Beneath ridges at shallow depths, carbonate-bearing silicate melts (basalts) are stable.[5,102,142] Melting in carbonated mantle lithologies may take place at depths of ~300 km[142] due to depression of the mantle solidus temperature.[5,29,157]

Figure 6.6 shows the stability fields of carbonates and carbonate and silicate melts in an adiabatically upwelling mantle and is compared with the fO_2 of the asthenospheric mantle. The fO_2 determined using reaction (6.10) suggests that carbonatitic melts are unstable at depths greater than 300 km due to the increased activity of Fe^{3+}-rich components in mantle minerals.[138,158,159] At the lower end of carbon concentrations in the mantle (30 ppm C for a MORB source mantle[54] and an initial $Fe^{3+}/\sum Fe$ content of 4%), graphite would transform to diamond at depths of ~160 km (Figure 6.2) and diamond would be the stable phase instead of carbonates or carbonatitic melts.[29,122,123] If the mantle is reduced below ~250 km depth and becomes metal saturated, then carbonatitic melts would be stable only to a depth of 150 km. During adiabatic upwelling of the upper mantle, reduction of Fe^{3+} locked in mantle silicates to Fe^{2+} results in concomitant oxidation of diamond or graphite and carbonatitic melting.[138] This redox process can be explained by reaction (6.12):

$$\underset{\text{graphite/diamond}}{C} + \underset{\text{silicate}}{2Fe_2O_3} = \underset{\text{carbonatitic melt}}{CO_2} + \underset{\text{silicate}}{4FeO} \quad (6.12)$$

As soon as 30 ppm of graphite in the upper mantle is oxidized, the $Fe^{3+}/\sum Fe$ content of the remaining mantle drops from 4% to 3%. After such redox melting, the fO_2 of the upper mantle increases again and finally reaches the level of mid-ocean ridge basalts at around FMQ (Figure 6.6).

6.9 Crustally Emplaced Carbonatites

Natural carbonate melts represent a tiny proportion of the magmatic rocks of Earth's crust, but nonetheless provide important insights into mantle-to-crust carbon transfer over geological time. Carbonate melts primarily refer to carbonatites, but could also include kimberlites and various other alkaline mafic–ultramafic silicate magma series (e.g.

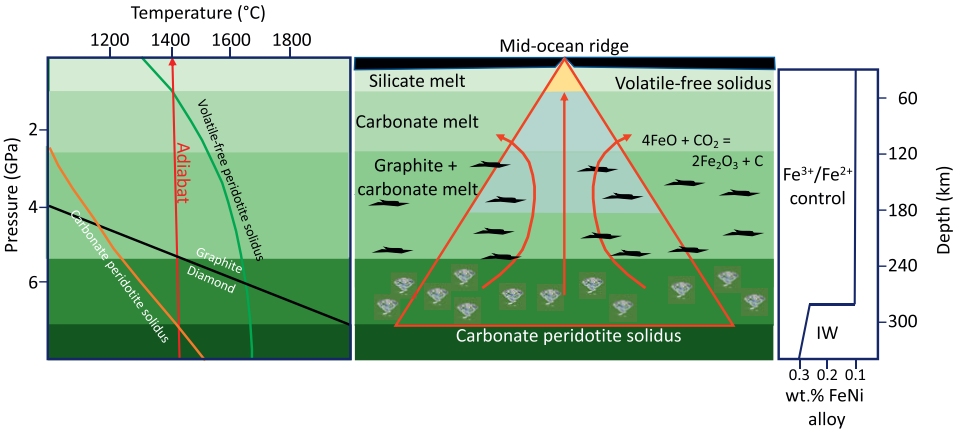

Figure 6.6 A simplified model for the extraction of carbonatitic/carbonated silicate melts from the mantle based on Stagno et al.[28] If carbonates are present in the adiabatically upwelling mantle beneath mid-ocean ridges, they will lower the melting temperature of the mantle rocks and melting will take place at ~300 km depth if the adiabat has a potential temperature of 1400°C. The left-hand panel shows that the solidus of peridotite and eclogite is depressed by several hundred degrees compared to the volatile-free solidus. The central panel shows the focusing of deeply derived carbonate melts (red triangle) formed by redox melting at about 1.5 GPa lower pressures than the carbonate peridotite solidus for oxidized mantle. The right-hand panel shows estimated $Fe^{3+}/\sum Fe$ in peridotite buffered at about 0.1 at depths below about 290 km, and buffered by FeNi alloy (≈IW) to higher values at greater depths.

lamprophyres). All of these magma types have indisputable mantle origins, as revealed by stable and radiogenic isotope signatures, as well as a common association with mantle-derived alkaline silicate magmas.[76]

Carbonatites (magmatic rocks with >50% carbonate minerals) are variably classified into a number of groups based on their chemistry, with most researchers agreeing on at least five groups; calcio-carbonatite, dolomite carbonatite, ferro-carbonatite, natro- (or alkali-) carbonatite, and rare earth carbonatites.[76] The Ca–Mg–Fe-rich carbonatites are primarily found as intrusive complexes that may to some extent represent crystal cumulates from carbonatite magma,[160] or as melt inclusions in igneous and mantle minerals.[161,162] Extrusive carbonatites are relatively rare in the rock record[163] and include the only known active carbonatite volcano, Oldoinyo Lengai (Tanzania), which erupts natrocarbonatite. Other occurrences of natrocarbonatite are found only very rarely as melt inclusions within igneous minerals from alkaline rocks[161,164] and kimberlites.[11] The lack of natrocarbonatite from the rock record is often ascribed to its extreme instability under atmospheric and most geological conditions.[165] Rare earth carbonatites (with >1 wt.% REE) also tend to be enriched in other incompatible trace elements (e.g. U, Th, Nb, Ta) and are regarded to be products of fractional crystallization of parental carbonatite magma.[166] This carbonatite class is of significant economic importance as a source of the critical metals needed for many technological applications that support modern societies.[167]

Despite consensus regarding their mantle origins, there are differing opinions on carbonatite evolution. Some researchers assert that carbonatites are primary magmas derived directly by low-degree melting of CO_2-rich mantle sources,[168] whereas experimental work by Watkinson and Wyllie[169] demonstrated that carbonate liquids could be formed as residua of fractionation from carbonated peralkaline silicate magmas; this latter origin would be consistent with the classification as "carbothermal residua" of Mitchell.[166] Supporting a primary mantle origin are studies of mantle xenoliths of distinctive petrological and geochemical character formed via metasomatism by carbonatitic melts.[8,76,170] Carbonatitic melt inclusions within diamond represent further unequivocal evidence of a mantle origin.[76,171]

A third origin proposed for carbonatite genesis is via liquid immiscibility from evolving CO_2-bearing alkaline silicate melts at crustal pressures.[76] Support for this model comes not only from experimental evidence and the common field association between carbonatite and alkaline silicate magmatic rocks, but crucially from a growing number of textural, petrological, and geochemical studies of carbonatites.[164,172–174] Given the compelling evidence for their primary mantle and immiscibility origins, it is likely that carbonatite magmas may be formed in a range of geological environments, from shallow crustal down to lower-mantle conditions.

Carbonatites and other mantle-derived CO_2-rich magmas, such as kimberlites, are found across all continents, although over half are in Africa.[175] They are most commonly found within Precambrian cratons despite the fact that most are of Phanerozoic age.[176,177] These settings would be consistent with formation via low-degree (and hence relatively low-temperature) melting of fertile mantle sources, such as thick mantle lithosphere beneath stable cratons. There tends to be an increasing frequency of their formation toward younger ages, which is not easily explained as an artefact of preservation,[177] but rather may reflect more favorable conditions for the production of mantle-derived alkaline magmatism in the modern Earth. This would be consistent with more effective recycling of crustal material into the mantle via modern-style subduction processes, allowing the production of the re-fertilized mantle domains that are requisite sources of these magmas.

There are diverse views on the tectonic settings in which carbonatites and other CO_2-bearing magmas form and are emplaced into the crust. Carbonatite magmatism is a distinctive feature of the recent igneous activity of the East African Rift, demonstrating a link to intracontinental rifting, and potentially mantle plumes.[178] Many older carbonatite complexes have also been linked to continental rifting, mantle plumes, or large igneous provinces.[179–181] However, Woolley and Bailey[177] argue that ephemeral mantle controls, such as mantle plumes, do not account for the episodic and repeated nature of carbonatitic (and kimberlitic) magmatism within restricted areas, sometimes over billions of years. Instead, these authors argue for reactivation of lithospheric-scale structures or lineaments due to far-field plate reorganization (e.g. due to rift initiation or continental assembly[182]), which allows for low-degree melting of the fertile cratonic mantle lithosphere to produce carbonatites or kimberlites, as well as efficient tapping of the melts to the surface.

Carbonatites in oceanic settings have only been described from the hot spot volcanos of Cape Verde and the Canary Islands.[183,184] In these settings, the degree of mantle melting is expected to be too high to produce carbonatites directly; rather, the carbonatites are

interpreted to be products of fractionation and unmixing from alkali-rich primitive basanite melts.[185] In this case, the rarity of oceanic carbonatites may reflect a lack of preservation and exposure rather than unsuitable petrogenesis conditions.

6.10 Concluding Remarks

The existence of carbonate-rich melts in Earth is likely limited in P–T–fO_2 space to the crust, to the uppermost part of the upper mantle including oceanic and continental lithosphere, to the mantle wedge above subducting slabs, to locally strongly metasomatized regions of the deep cratonic lithospheric mantle and asthenosphere, and to local regions of the deep upper mantle, mantle transition zone, and uppermost lower mantle associated with deep subduction of the carbonate-bearing oceanic lithosphere. Much of the deep Earth is too reduced for carbonate or carbonate-rich melts to be stable, where carbon will exist in reduced forms, such as diamond, methane, and other alkanes or volatile organic molecules, as well as Fe-carbides.

Despite this, carbonate melts are of tremendous importance as agents of mass transport and metasomatic enrichment in Earth's interior. They are also the primary source of almost all commercially viable REE resources, and they may contain other critical metals in extractable quantities as well. Although crustally emplaced carbonatites are small in volume, they are likely to be much more abundant as broadly alkali-rich calcio-dolomitic to dolomitic melts in the upper mantle and mantle transition zone, where they contribute significantly to the carbon fluxes to the surface.

6.11 Limits to Knowledge and Unknowns

Key areas relating to carbonate or CO_2-bearing melts in Earth in which current knowledge is limited include the solubility of CO_2 in hydrous fluids and partial melts derived from subducting oceanic crust, particularly in the sub-arc environment. These melts may play a critically important role in metasomatizing the mantle wedge and flux melting, ultimately leading to arc volcanism and continental crust formation. They are agents by which subducted carbon is recycled on relatively short timescales of tens of Ma from the subducted slab in the sub-arc environment (blueschist or eclogite facies conditions) back to the atmosphere and hydrosphere. We cannot quantify carbon fluxes in this relatively shallow part of Earth's deep carbon cycle unless we understand the magnitude of volatile fluxes from slab to arc volcanism. This will require high-pressure experimental studies as well as field studies of high-grade, carbonated metamorphic rocks in orogenic zones.

This in turn bears on estimates of carbon fluxes via subduction into the deeper mantle, and ultimately to the mantle transition zone or lower mantle. These estimates currently vary from 0 to 15 Mt/year.[56] It appears likely that some carbon does escape relatively shallow recycling during subduction to sub-arc conditions based on studies of sublithospheric diamonds and their inclusions. If so, it may then be transported as part of the oceanic lithosphere to the deeper mantle. However, it remains unclear how the fO_2 of the oceanic crustal components being subducted as part of the lithospheric package varies along the prograde path. This will

be a critical control on the ultimate fate of carbon in the oceanic crust. For example, as has been shown recently by Kiseeva et al.[12] and Thomson et al.,[13] carbonate in the mafic crust is unlikely to be subducted beyond the mantle transition zone, as it will melt to form carbonate liquids, which will segregate from their source and undergo redox freezing on contact with reduced peridotite wall-rock.[138] However, if carbonate is reduced to diamond on the prograde path, melting will not occur, and in those cases where slabs enter the lower mantle, carbon will likely also be transported beyond the mantle transition zone.

Finally, we currently lack understanding of aspects of the return cycle of carbon from the deep upper mantle, mantle transition zone, or lower mantle to the surface. In particular, some sublithospheric diamonds originate from these very deep parts of the upper and lower mantle based on their mineral inclusions. However, it is unclear exactly how and where the kimberlites formed that host these diamonds and transported them to the surface. Did they form at deep upper-mantle, transition-zone, or lower-mantle pressures, or were the sub-lithospheric diamonds first transported from great depths during mantle convection and then entrained in kimberlites formed at depths just below the cratonic lithospheric mantle? Answering these questions will require careful high-pressure experimental studies in order to deepen understanding of the role of C–O–H volatiles in causing melting at depths in and around the transition zone.

Acknowledgments

We gratefully thank the editorial team for this book, Beth Orcutt, Isabelle Daniel, and Raj Dasgupta, for their encouragement and immense patience in the development of this chapter and for their expert editorial handling. We also thank Raj Dasgupta and an anonymous reviewer for two constructive formal reviews.

Questions for the Classroom

1 Describe the different forms in which carbon is believed to exist in Earth's mantle. In which parts of the mantle are these different carbon-bearing species located and what is the evidence for their presence?
2 Explain how pressure, temperature, and fO_2 in Earth's mantle influence the species present in different parts of the mantle (lower mantle, mantle transition zone, upper mantle) and different tectonic settings.
3 What are some of the reasons that carbonate melts inferred to exist in parts of the subcontinental lithosphere are considered to be highly effective metasomatic agents?
4 Carbonate is a widespread component of oceanic crust hydrothermally altered near mid-ocean ridges. When transported by plate tectonics to subduction zones, this carbonate may be recycled back into the mantle. Describe some of the processes that may influence the fate and redistribution of this subducted carbon in the fore-arc, sub-arc, and deeper environments.

5 How does fO_2 vary within Earth's mantle? What are the major controls on this variation and why is it important in understanding Earth's deep carbon cycle?
6 Sublithospheric diamonds are believed to have formed at depths greater than the lithosphere–asthenosphere boundary (i.e. they did not form within the cratonic mantle lithosphere like the majority of kimberlite-borne diamonds). From where are they derived and how are they likely to have formed? What is the evidence for this?
7 The only currently active carbonatite volcano on Earth is Oldoinyo Lengai in Tanzania. How are the carbonatites erupted by this volcano different from all other known crustally emplaced carbonatites? Do some literature research to understand some of the hypotheses for the formation of Oldoinyo Lengai's lavas and the possible reasons that they are so anomalous relative to other older carbonatites.
8 What are the likely reasons for the absence of crustally emplaced carbonatite melts in subduction zones?
9 Describe ways in which CO_2-rich silicate melts can form in Earth's upper mantle. In what sorts of tectonic settings are these melts likely to erupt?
10 Draw a cross-section of Earth showing the main tectonic settings (e.g. mid-ocean ridge, subduction zone, intraplate volcanic setting, continental and cratonic setting, etc.) and illustrate the locations of major carbon reservoirs and the nature of the carbon-bearing species that may be present in each. Discuss processes by which carbon may move between these reservoirs.

References

1. Dawson, J. B. Sodium carbonate lavas from Oldoinyo Lengai, Tanganyika. *Nature* **195**, 1075 (1962).
2. Wyllie, P. J., Baker, M. B. & White, B. S. Experimental boundaries for the origin and evolution of carbonatites. *Lithos* **26**, 3–19 (1990).
3. Wallace, M. E. & Green, D. H. An experimental-determination of primary carbonatite magma composition. *Nature* **335**, 343–346 (1988).
4. Yaxley, G. & Brey, G. Phase relations of carbonate-bearing eclogite assemblages from 2.5 to 5.5 GPa: implications for petrogenesis of carbonatites. *Contrib Mineral Petrol* **146**, 606–619 (2004).
5. Dasgupta, R. & Hirschmann, M. M. Melting in the Earth's deep upper mantle caused by carbon dioxide. *Nature* **440**, 659–662 (2006).
6. Dasgupta, R. & Hirschmann, M. M. The deep carbon cycle and melting in Earth's interior. *Earth Planet Sci Lett* **298**, 1–13 (2010).
7. Yaxley, G., Crawford, A. & Green, D. Evidence for carbonatite metasomatism in spinel peridotite xenoliths from western Victoria, Australia. *Earth Planet Sci Lett* **107**, 305–317 (1991).
8. Yaxley, G., Green, D. & Kamenetsky, V. Carbonatite metasomatism in the southeastern Australian lithosphere. *J Petrol* **39**, 1917–1930 (1998).
9. Rudnick, R. L., Mcdonough, W. F. & Chappell, B. W. Carbonatite metasomatism in the northern Tanzanian mantle – petrographic and geochemical characteristics. *Earth Planet Sci Lett* **114**, 463–475 (1993).

10. Weiss, Y., McNeill, J., Pearson, D. G., Nowell, G. M. & Ottley, C. J. Highly saline fluids from a subducting slab as the source for fluid-rich diamonds. *Nature* **524**, 339–342 (2015).
11. Golovin, A. V., Sharygin, I. S., Kamenetsky, V. S., Korsakov, A. V. & Yaxley, G. M. Alkali-carbonate melts from the base of cratonic lithospheric mantle: links to kimberlites. *Chem Geol* **483**, 261–274 (2018).
12. Kiseeva, E. S., Litasov, K. D., Yaxley, G. M., Ohtani, E. & Kamenetsky, V. S. Melting and phase relations of carbonated eclogite at 9-21 GPa and the petrogenesis of alkali-rich melts in the deep mantle. *J Petrol* **54**, 1555–1583 (2013).
13. Thomson, A. R., Walter, M. J., Kohn, S. C. & Brooker, R. A. Slab melting as a barrier to deep carbon subduction. *Nature* **529**, 76–79 (2016).
14. Litasov, K. & Ohtani, E. Solidus of carbonate eclogite in the system $CaO–Al_2O_3–MgO–SiO_2–Na_2O–CO_2$ to 32 GPa and carbonatite liquid in the deep mantle. *Earth Planet Sci Lett* **295,** 115–126 (2010).
15. Kaminsky, F. Mineralogy of the lower mantle: a review of "super-deep" mineral inclusions in diamond. *Earth Sci Rev* **110**, 127–147 (2012).
16. Hunter, R. H. & Mckenzie, D. The equilibrium geometry of carbonate melts in rocks of mantle composition. *Earth Planet Sci Lett* **92**, 347–356 (1989).
17. Hammouda, T. & Laporte, D. Ultrafast mantle impregnation by carbonatite melts. *Geology* **28**, 283–285 (2000).
18. Shatskiy, A. et al. Silicate diffusion in alkali-carbonatite and hydrous melts at 16.5 and 24 GPa: implication for the melt transport by dissolution–precipitation in the transition zone and uppermost lower mantle. *Phys Earth Planet Int* **225**, 1–11 (2013).
19. Taylor, W. R. & Green, D. H. The petrogenic role of methane: effect on liquidus phase relations and the solubility mechanism of reduced C–H volatiles. *The Geochemical Society* **Special Publication No. 1**, 121–137 (1987).
20. Luth, R. W. Diamonds, eclogites, and the oxidation-state of the Earth's mantle. *Science* **261**, 66–68 (1993).
21. Stagno, V., Ojwang, D. O., McCammon, C. A. & Frost, D. J. The oxidation state of the mantle and the extraction of carbon from Earth's interior. *Nature* **493**, 84–88 (2013).
22. Kennedy, C. S. & Kennedy, G. C. The equilibrium boundary between graphite and diamond. *J Geophys Res* **81**, 2467–2470 (1976).
23. Yaxley, G. M., Berry, A. J., Rosenthal, A., Woodland, A. B. & Paterson, D. Redox preconditioning deep cratonic lithopshere for kimberlite genesis – evidence from the central Slave Craton. *Nat Sci Rep* **7,** 30 (2017).
24. Kiseeva, E. S. et al. Oxidized iron in garnets from the mantle transition zone. *Nat Geosci* **11,** 144–147 (2018).
25. Cottrell, E. & Kelley, K. A. The oxidation state of Fe in MORB glasses and the oxygen fugacity of the upper mantle. *Earth Planet Sci Lett* **305**, 270–282, (2011).
26. Berry, A. J., Stewart, G. A., O'Neill, H. S. C., Mallmann, G. & Mosselmans, J. F. W. A re-assessment of the oxidation state of iron in MORB glasses. *Earth Planet Sci Lett* **483**, 114–123 (2018).
27. Gudmundsson, G. & Wood, B. J. Experimental tests of garnet peridotite oxygen barometry. *Contrib Mineral Petrol* **119**, 56–67 (1995).
28. Stagno, V., Frost, D. J., McCammon, C. A., Mohseni, H. & Fei, Y. The oxygen fugacity at which graphite or diamond forms from carbonate-bearing melts in eclogitic rocks. *Contrib Mineral Petrol* **169**, 16 (2015).
29. Stagno, V. & Frost, D. J. Carbon speciation in the asthenosphere: experimental measurements of the redox conditions at which carbonate-bearing melts coexist with

graphite or diamond in peridotite assemblages. *Earth Planet Sci Lett* **300**, 72–84 (2010).
30. Falloon, T. J. & Green, D. H. The solidus of carbonated, fertile peridotite. *Earth Planet Sci Lett* **94**, 364–370 (1989).
31. Falloon, T. J. & Green, D. H. Solidus of carbonated fertile peridotite under fluid-saturated conditions. *Geology* **18**, 195–199 (1990).
32. Dasgupta, R. & Hirschmann, M. M. Effect of variable carbonate concentration on the solidus of mantle peridotite. *Am Mineral* **92**, 370–379 (2007).
33. Dasgupta, R., Hirschmann, M. M. & Smith, N. D. Partial melting experiments of peridotite + CO_2 at 3 GPa and genesis of alkalic ocean island basalts. *J. Petrol* **48**, 2093–2124 (2007).
34. Dasgupta, R., Hirschmann, M. M. & Smith, N. D. Water follows carbon: CO_2 incites deep silicate melting and dehydration beneath mid-ocean ridges. *Geology* **35**, 135–138 (2007).
35. Dasgupta, R., Stalker, K., Withers, A. C. & Hirschmann, M. M. The transition from carbonate-rich to silicate-rich melts in eclogite: partial melting experiments of carbonated eclogite at 3 GPa. *Lithos* **73**, S23 (2004).
36. Lee, W. J. & Wyllie, P. J. Petrogenesis of carbonatite magmas from mantle to crust, constrained by the system CaO–(MgO+FeO*)(Na_2O+K_2O)–(SiO_2+Al_2O_3+TiO_2)–CO_2. *J Petrol* **39**, 495–517 (1998).
37. Ryabchikov, I. D., Edgar, A. D. & Wyllie, P. J. Partial melting in the systen carbonate phosphate peridotite at 30 kbar. *Geokhimiya* **2**, 163–168 (1991).
38. White, B. S. & Wyllie, P. J. Solidus reactions in synthetic lherzolite–H_2O–CO_2 from 20–30kbar, with applications to melting and metasomatism. *J Volcanol Geoth Res* **50**, 117–130 (1992).
39. Wyllie, P. J. Peridotite–CO_2–H_2O and carbonatitic liquids in upper asthenosphere. *Nature* **266**, 45–47 (1977).
40. Wyllie, P. J. Mantle fluid compositions buffered in peridotite–CO_2–H_2O by carbonates, amphibole, and phlogopite. *J Geol* **86**, 687–713 (1978).
41. Wyllie, P. J. Fusion of peridotite–H_2O–CO_2 in system peridotite–H–C–O at upper mantle pressures. *Eos Trans Am Geophysl Union* **59**, 398–398 (1978).
42. Newton, R. C. & Sharp, W. E. Stability of forsterite + CO_2 and its bearing on the role of CO_2 in the mantle. *Earth Planet Sci Lett* **26**, 239–244 (1975).
43. Haselton, H. T., Sharp, W. E. & Newton, R. C. CO_2 fugacity at high temeratures and pressures from experimental decarbonation reactions. *Geophys Res Lett* **5**, 753 (1978).
44. Eggler, D. H., Kushiro, J. & Holloway, J. R. Free energies of decarbonation reactions at mantle pressures, I. Stability of the assemblage forsterite-enstatite-magnesite in the system MgO–SiO_2–CO_2–H_2O to 60 kbar. *Am Mineral* **64**, 288 (1979).
45. Johannes, W. An experimental investigation of the system MgO–SiO_2–H_2O–CO_2. *Am J Sci* **267**, 1083 (1969).
46. Wyllie, P. J. Magmass and volatile components. *Am Mineral* **64**, 469–500 (1979).
47. Eggler, D. H. The effect of CO_2 on partial melting of peridotite in the system Na_2O–CaO–Al_2O_3–MgO–SiO_2–CO_2 to 35 kbar, with an analysis of melting in a peridotite–H_2O–CO_2 system. *Am J Sci* **278**, 305 (1978).
48. Kushiro, I. Carbonate–silicate reactions at high presures and possible presence of dolomite and magnesite in the upper mantle. *Earth Planet Sci Lett* **28**, 116–120(1975).
49. Brey, G. et al. Pyroxene–carbonate reactions in the upper mantle. *Earth Planet Sci Lett* **62**, 63–74 (1983).

50. Yaxley, G. M., Crawford, A. J. & Green, D. H. Evidence for carbonatite metasomatism in spinel peridotite xenoliths from Western Victoria, Australia. *Earth Planet Sci Lett* **107**, 305–317 (1991).
51. Rudnick, R. L., McDonough, W. F. & Chappell, B. W. Carbonatite metasomatism in the northern Tanzanian mantle: petrographic and geochemical characteristics. *Earth Planet Sci Lett* **114**, 463–475 (1993).
52. Dalton, J. A. & Wood, B. J. The compositions of primary carbonate melts and their evolution through wallrock reaction in the mantle. *Earth Planet Sci Lett* **119**, 511–525 (1993).
53. Foley, S. F. et al. The composition of near-solidus melts of peridotite in the presence of CO_2 and H_2O between 40 and 60 kbar. *Lithos* **112**, 274–283 (2009).
54. Marty, B. The origins and concentrations of water, carbon, nitrogen and noble gases on Earth. *Earth Planet Sci Lett* **313–314**, 56–66 (2012).
55. Sleep, N. H. & Zahnle, K. Carbon dioxide cycling and implications for climate on ancient Earth. *J Geophys Res Planets* **106**, 1373–1399 (2001).
56. Kelemen, P. B. & Manning, C. E. Reevaluating carbon fluxes in subduction zones, what goes down, mostly comes up. *Proc Natl Acad Sci* **112**, E3997–E4006 (2015).
57. Plank, T. & Langmuir, C. H. The chemical composition of subducting sediment and its consequences for the crust and mantle. *Chem Geol* **145**, 325–394 (1998).
58. Plank, T. The chemical composition of subducting sediments. *Treatise Geochem* **4**, 607–629 (2014).
59. Alt, J. C. & Teagle, D. A. H. The uptake of carbon during alteration of ocean crust. *Geochim Cosmochim Acta* **63**, 1527–1535 (1999).
60. Connolly, J. A. D. Computation of phase equilibria by linear programming; a tool for geodynamic modelling and its application to subduction zone decarbonation. *Earth Planet Sci Lett* **236**, 524–541 (2005).
61. Manning, C. E., Shock, E. L. & Sverjensky, D. A. The chemistry of carbon in aqueous fluids at crustal and upper-mantle conditions: experimental and theoretical constraints. *Rev Mineral Geochem* **75**, 109–148 (2013).
62. Ague, J. J. & Nicolescu, S. Carbon dioxide released from subduction zones by fluid-mediated reactions. *Nat Geosci* **7**, 355 (2014).
63. Piccoli, F. et al. Carbonation by fluid–rock interactions at high-pressure conditions: implications for carbon cycling in subduction zones. *Earth Planet Sci Lett* **445**, 146–159 (2016).
64. Spandler, C., Hermann, J., Faure, K., Mavrogenes, J. A. & Arculus, R. J. The importance of talc and chlorite "hybrid" rocks for volatile recycling through subduction zones; evidence from the high-pressure subduction mélange of New Caledonia. *Contrib Mineral Petrol* **155**, 181–198 (2008).
65. Scambelluri, M. et al. Carbonation of subduction-zone serpentinite (high-pressure ophicarbonate; Ligurian Western Alps) and implications for the deep carbon cycling. *Earth Planet Sci Lett* **441**, 155–166 (2016).
66. Sieber, M. J., Hermann, J. & Yaxley, G. M. An experimental investigation of C–O–H fluid-driven carbonation of serpentinites under forearc conditions. *Earth Planet Sci Lett* **496**, 178–188 (2018).
67. Syracuse, E. M., van Keken, P. E. & Abers, G. A. The global range of subduction zone thermal models. *Phys Earth Planet Interiors* **183**, 73–90 (2010).
68. Frezzotti, M. L., Selverstone, J., Sharp, Z. D. & Compagnoni, R. Carbonate dissolution during subduction revealed by diamond-bearing rocks from the Alps. *Nat Geosci* **4**, 703 (2011).

69. Schmidt, M. W. Melting of pelitic sediments at subarc depths: 2. Melt chemistry, viscosities and a parameterization of melt composition. *Chem Geol* **404**, 168–182 (2015).
70. Korsakov, A. V. & Hermann, J. Silicate and carbonate melt inclusions associated with diamonds in deeply subducted carbonate rocks. *Earth Planet Sci Lett* **241**, 104–118 (2006).
71. Poli, S. Carbon mobilized at shallow depths in subduction zones by carbonatitic liquids. *Nat Geosci* **8**, 633 (2015).
72. Marschall, H. R. & Schumacher, J. C. Arc magmas sourced from melange diapirs in subduction zones. *Nat Geosci* **5**, 862–867 (2012).
73. Tumiati, S., Fumagalli, P., Tiraboschi, C. & Poli, S. An experimental study on COH-bearing peridotite up to 3.2 GPa and implications for crust–mantle recycling. *J Petrol* **54**, 453–479 (2013).
74. Smith, C. B. et al. Diamonds from Dachine, French Guiana: a unique record of early Proterozoic subduction. *Lithos* **265**, 82–95 (2016).
75. Green, D. H. Experimental petrology of peridotites, including effects of water and carbon on melting in the Earth's upper mantle. *Phys Chem Mineral* **42**, 95–122 (2015).
76. Jones, A. P., Genge, M. & Carmody, L. Carbonate melts and carbonatites. *Rev Mineral Geochem* **75**, 289–322 (2013).
77. Saha, S., Dasgupta, R. & Tsuno, K. High pressure phase relations of a depleted peridotite fluxed by CO_2–H_2O-bearing siliceous melts and the origin of Mid-Lithospheric Discontinuity. *Geochem Geophys Geosyst* **19**, 595–620 (2018).
78. Gorman, P. J., Kerrick, D. M. & Connolly, J. A. D. Modeling open system metamorphic decarbonation of subducting slabs. *Geochem Geophys Geosyst* **7**, 1–21 (2006).
79. Molina, J. F. & Poli, S. Carbonate stability and fluid composition in subducted oceanic crust: an experimental study on H_2O–CO_2-bearing basalts. *Earth Planet Sci Lett* **176**, 295–310 (2000).
80. Kelley, K. A. & Cottrell, E. The influence of magmatic differentiation on the oxidation state of Fe in a basaltic arc magma. *Earth Planet Sci Lett* **329–330**, 109–121 (2012).
81. Brenker, F. E. et al. Carbonates from the lower part of transition zone or even the lower mantle. *Earth Planet Sci Lett* **260**, 1–9 (2007).
82. Bulanova, G. P. et al. Mineral inclusions in sublithospheric diamonds from Collier 4 kimberlite pipe, Juina, Brazil: subducted protoliths, carbonated melts and primary kimberlite magmatism. *Contrib Mineral Petrol* **160**, 489–510 (2010).
83. Thomson, A. R. et al. Origin of sub-lithospheric diamonds from the Juina-5 kimberlite (Brazil): constraints from carbon isotopes and inclusion compositions. *Contrib Mineral Petrol* **168**, 1081 (2014).
84. Zedgenizov, D. A., Kagi, H., Shatsky, V. S. & Ragozin, A. L. Local variations of carbon isotope composition in diamonds from Sao-Luis (Brazil): evidence for heterogenous carbon reservoir in sublithospheric mantle. *Chem Geol* **363**, 114–124 (2010).
85. Thomson, A. R. et al. Trace element composition of silicate inclusions in sub-lithospheric diamonds from the Juina-5 kimberlite: evidence for diamond growth from slab melts. *Lithos* **265**, 108–124 (2016).
86. Walter, M. J. et al. Primary carbonatite melt from deeply subducted oceanic crust. *Nature* **454**, 622 (2008).
87. Burnham, A. D. et al. Stable isotope evidence for crustal recycling as recorded by superdeep diamonds. *Earth Planet Sci Lett* **432**, 374–380 (2015).

88. Ickert, R. B., Stachel, T., Stern, R. A. & Harris, J. W. Diamond from recycled crustal carbon documented by coupled $\delta^{18}O$–$\delta^{13}C$ measurements of diamonds and theirinclusions. *Earth Planet Sci Lett* **364**, 85–97 (2013).
89. Tsuno, K. & Dasgupta, R. Melting phase relation of nominally anhydrous, carbonated pelitic-eclogite at 2.5–3.0 GPa and deep cycling of sedimentary carbon. *Contrib Mineral Petrol* **161**, 743–763 (2011).
90. Grassi, D. & Schmidt, M. W. Melting of carbonated pelites at 8-13 GPa: generating K-rich carbonatites for mantle metasomatism. *Contrib Mineral Petrol* **162**, 169–191 (2011).
91. Mann, U. & Schmidt, M. W. Melting of pelitic sediments at subarc depths: 1. Flux vs. fluid-absent melting and a parameterization of melt productivity. *Chem Geol* **404**, 150–167 (2015).
92. Keshav, S. & Gudfinnsson Gudmundur, H. Experimentally dictated stability of carbonated oceanic crust to moderately great depths in the Earth: results from the solidus determination in the system CaO–MgO–Al_2O_3–SiO_2–CO_2. *J Geophys Res Solid Earth* **115**, B05205 (2010).
93. Litasov, K. & Ohtani, E. The solidus of carbonated eclogite in the system CaO–Al_2O_3–MgO–SiO_2–Na_2O–CO_2 to 32GPa and carbonatite liquid in the deep mantle. *Earth Planet Sci Lett* **295**, 115–126 (2010).
94. Dasgupta, R., Hirschmann, M. M. & Withers, A. C. Deep global cycling of carbon constrained by the solidus of anhydrous, carbonated eclogite under upper mantle conditions. *Earth Planet Sci Lett* **227**, 73–85 (2004).
95. Hammouda, T. High-pressure melting of carbonated eclogite and experimental constraints on carbon recycling and storage in the mantle. *Earth Planet Sci Lett* **214**, 357–368 (2003).
96. Kiseeva, E. S. et al. An experimental study of carbonated eclogite at 3.5–5.5 GPa – implications for silicate and carbonate metasomatism in the cratonic mantle. *J Petrol* **53**, 727–759 (2012).
97. Yaxley, G. M. & Green, D. H. Experimental demonstration of refractory carbonate-bearing eclogite and siliceous melt in the subduction regime. *Earth Planet Sci Lett* **128**, 313–325 (1994).
98. Dasgupta, R., Hirschmann, M. M. & Dellas, N. The effect of bulk composition on the solidus of carbonated eclogite from partial melting experiments at 3 GPa. *Contrib Mineral Petrol* **149**, 288–305 (2005).
99. Gerbode, C. & Dasgupta, R. Carbonate-fluxed melting of MORB-like pyroxenite at 2.9 GPa and genesis of HIMU ocean island basalts. *J Petrol* **51**, 2067–2088 (2010).
100. Dasgupta, R., Hirschmann, M. M. & Stalker, K. Immiscible transition from carbonate-rich to silicate-rich melts in the 3 GPa melting interval of eclogite + CO_2 and genesis of silica-undersaturated ocean island lavas. *J Petrol* **47**, 647–671 (2006).
101. Litasov, K. D., Shatskiy, A., Ohtani, E. & Yaxley, G. M. Solidus of alkaline carbonatite in the deep mantle. *Geology* **41**, 79–82 (2013).
102. Gudfinnsson, G. H. & Presnall, D. C. Continuous gradations among primary carbonatitic, kimberlitic, melilititic, basaltic, picritic, and komatiitic melts in equilibrium with garnet lherzolite at 3–8GPa. *J Petrol* **46**, 1645–1659 (2005).
103. Tappe, S., Foley, S. F., Jenner, G. A. & Kjarsgaard, B. A. Integrating ultramafic lamprophyres into the IUGS classification of igneous rocks: rationale and implications. *J Petrol* **46**, 1893–1900 (2005).

104. Tappe, S. et al. Between carbonatite and lamproite – diamondiferous Torngat ultramafic lamprophyres formed by carbonate-fluxed melting of cratonic MARID-type metasomes. *Geochim Cosmochim Acta* **72**, 3258–3286 (2008).
105. Sparks, R. S. J. Kimberlite volcanism. *Ann Rev Earth Planet Sci* **41**, 497–528 (2013).
106. Mitchell, R. H. *Kimberlites, Orangeites, and Related Pocks* (Plenum Press, 1995).
107. Becker, M. & Le Roex, A. P. Geochemistry of South African on- and off-craton, Group I and Group II kimberlites: petrogenesis and source region evolution. *J Petrol* **47**, 673–703 (2006).
108. Mitchell, R. H. Kimberlites and lamproites – primary sources of diamond. *Geosci Canada* **18**, 1–16 (1991).
109. Nowell, G. M. et al. Hf isotope systematics of kimberlites and their megacrysts: new constraints on their source regions. *J Petrol* **45**, 1583–1612 (2004).
110. Yaxley, G. M. et al. The discovery of kimberlites in Antarctica extends the vast Gondwanan Cretaceous province. *Nat Commun* **4**, 2921 (2013).
111. Novella, D. & Frost, D. J. The composition of hydrous partial melts of garnet peridotite at 6 GPa: implications for the origin of Group II kimberlites. *J Petrol* **55**, 2097–2124 (2014).
112. Foley, S. F. & Fischer, T. P. An essential role for continental rifts and lithosphere in the deep carbon cycle. *Nat Geosci* **10**, 897–902 (2017).
113. Patterson, M., Francis, D. & McCandless, T. Kimberlites: magmas or mixtures? *Lithos* **112**, 191–200 (2009).
114. Kamenetsky, M. B. et al. Kimberlite melts rich in alkali chlorides and carbonates: a potent metasomatic agent in the mantle. *Geology* **32**, 845–848 (2004).
115. Kamenetsky, V. S. et al. Olivine in the Udachnaya-East kimberlite (Yakutia, Russia): types, compositions and origins. *J Petrol* **49**, 823–839 (2008).
116. Russell, J. K., Porritt, L. A., Lavallee, Y. & Dingwell, D. B. Kimberlite ascent by assimilation-fuelled buoyancy. *Nature* **481**, 352–356 (2012).
117. Girnis, A. V., Brey, G. P. & Ryabchikov, I. D. Origin of Group 1A kimberlites: fluid-saturated melting experiments at 45–55 kbar. *Earth Planet Sci Lett* **134**, 283–296 (1995).
118. Girnis, A. V., Bulatov, V. K. & Brey, G. P. Formation of primary kimberlite melts – constraints from experiments at 6–12GPa and variable CO_2/H_2O. *Lithos* **127**, 401–413 (2011).
119. Nell, J. & Wood, B. J. High-temperature electrical measurements and thermodynamic properties of Fe_3O_4–$FeCr_2O_4$–$MgCr_2O_4$–$FeAl_2O_4$ spinels. *Am Mineral* **76**, 405–426 (1991).
120. Ballhaus, C., Berry, R. F. & Green, D. H. High-pressure experimental calibration of the olivine–ortho-pyroxene–spinel oxygen geobarometer – implications for the oxidation-state of the upper mantle. *Contrib Mineral Petrol* **107**, 27–40 (1991).
121. O'Neill, H. S. C. & Wall, V. J. The olivine–orthopyroxene–spinel oxygen geobarometer, the nickel precipitation curve, and the oxygen fugacity of the Earth's upper mantle. *J Petrol* **28**, 1169–1191 (1987).
122. Woodland, A. B. & Koch, M. Variation in oxygen fugacity with depth in the upper mantle beneath the Kaapvaal craton, Southern Africa. *Earth Planet Sci Lett* **214**, 295–310 (2003).
123. Yaxley, G. M., Berry, A. J., Kamenetsky, V. S., Woodland, A. B. & Golovin, A. V. An oxygen fugacity profile through the Siberian Craton–Fe K-edge XANES determinations of $Fe^{3+}/\sum$ Fe in garnets in peridotite xenoliths from the Udachnaya East kimberlite. *Lithos* **140**, 142–151 (2012).

124. Frost, D. J. & McCammon, C. A. The redox state of Earth's mantle. *Ann Rev Earth Planet Sci* **36**, 389–420 (2008).
125. Rohrbach, A., Ghosh, S., Schmidt, M. W., Wijbrans, C. H. & Klemme, S. The stability of Fe–Ni carbides in the Earth's mantle: evidence for a low Fe–Ni–C melt fraction in the deep mantle. *Earth Planet Sci Lett* **388**, 211–221 (2014).
126. Tsuno, K. & Dasgupta, R. Fe–Ni–Cu–C–S phase relations at high pressures and temperatures – the role of sulfur in carbon storage and diamond stability at mid- to deep-upper mantle. *Earth Planet Sci Lett* **412**, 132–142 (2015).
127. Yaxley, G. M., Berry, A. J., Kamenetsky, V. S., Woodland, A. B. & Golovin, A. V. An oxygen fugacity profile through the Siberian Craton; Fe K-edge XANES determinations of $Fe^{3+}/\sum Fe$ in garnets in peridotite xenoliths from the Udachnaya East kimberlite. *Lithos* **140–141**, 142–151 (2012).
128. Foley, S. F. Rejuvenation and erosion of the cratonic lithosphere. *Nat Geosci* **1**, 503–510 (2008).
129. Coltorti, M., Beccaluva, L., Bonadiman, C., Salvini, L. & Siena, F. Glasses in mantle xenoliths as geochemical indicators of metasomatic agents. *Earth Planet Sci Lett* **183**, 303–320 (2000).
130. Delpech, G. et al. Feldspar from carbonate-rich silicate metasomatism in the shallow oceanic mantle under Kerguelen Islands (South Indian Ocean). *Lithos* **75**, 209–237 (2004).
131. Misra, K. C., Anand, M., Taylor, L. A. & Sobolev, N. V. Multi-stage metasomatism of diamondiferous eclogite xenoliths from the Udachnaya kimberlite pipe, Yakutia, Siberia. *Contrib Mineral Petrol* **146**, 696–714 (2004).
132. Taylor, W. R. & Green, D. H. Measurement of reduced peridotite–C–O–H solidus and implications for redox melting of the mantle. *Nature* **332**, 349–352 (1988).
133. Litasov, K. D., Shatskiy, A. & Ohtani, E. Melting and subsolidus phase relations in peridotite and eclogite systems with reduced COH fluid at 3–16 GPa. *Earth Planet Sci Lett* **391**, 87–99 (2014).
134. Eguchi, J. & Dasgupta, R. Redox state of the convective mantle from CO_2-trace element systematics of oceanic basalts. *Geochem Perspect Lett* **8**, 7–21 (2018).
135. Kogarko, L. N., Henderson, C. M. B. & Pacheco, H. Primary Ca-rich carbonatite magma and carbonate–silicate–sulfide liquid immiscibility in the upper-mantle. *Contrib Mineral Petrol* **121**, 267–274 (1995).
136. Schiano, P., Clocchiatti, R., Shimizu, N., Weis, D. & Mattielli, N. Cogenetic silica-rich and carbonate-rich melts trapped in mantle minerals in Kerguelen ultramafic xenoliths – implications for metasomatism in the oceanic upper-mantle. *Earth Planet Sci Lett* **123**, 167–178 (1994).
137. Dixon, J., Clague David, A., Cousens, B., Monsalve Maria, L. & Uhl, J. Carbonatite and silicate melt metasomatism of the mantle surrounding the Hawaiian plume: evidence from volatiles, trace elements, and radiogenic isotopes in rejuvenated-stage lavas from Niihau, Hawaii. *Geochem Geophys Geosyst* **9**, 9 (2008).
138. Rohrbach, A. & Schmidt, M. W. Redox freezing and melting in the Earth's deep mantle resulting from carbon-iron redox coupling. *Nature* **472**, 209–212, (2011).
139. Dasgupta, R. Volatile-bearing partial melts beneath oceans and continents – where, how much and of what compositions. *Am J Sci* **318**, 141–165 (2018).
140. Eguchi, J. & Dasgupta, R. CO_2 content of andesitic melts at graphite-saturated upper mantle conditions with implications for redox state of oceanic basalt source regions and remobilization of reduced carbon from subducted eclogite. *Contrib Mineral Petrol* **172**, 12 (2017).

141. Dalton, J. A. & Presnall, D. C. Carbonatitic melts along the solidus of model lherzolite in the system CaO–MgO–Al_2O_3–SiO_2–CO_2 from 3 to 7 GPa. *Contrib Mineral Petrol* **131**, 123–135 (1998).
142. Dasgupta, R. et al. Carbon-dioxide-rich silicate melt in the Earth's upper mantle. *Nature* **493**, 211–215 (2013).
143. Green, D. H. & Wallace, M. E. Mantle metasomatism by ephemeral carbonatite melts. *Nature* **336**, 459–462 (1988).
144. Keshav, S. & Gudfinnsson, G. H. Melting phase equilibria of model carbonated peridotite from 8 to 12 GPa in the system CaO–MgO–Al_2O_3–SiO_2–CO_2 and kimberlitic liquids in the Earth's upper mantle. *Am Mineral* **99**, 1119–1126 (2014).
145. Mysen, B. O. & Boettcher, A. L. Melting of a hydrous mantle: I. Phase relations of natural peridotite at high pressures and temperatures with controlled activities of water, carbon dioxide, and hydrogen. *J Petrol* **16**, 520–548 (1975).
146. Wendlandt, R. F. & Mysen, B. O. Melting relations of natural peridotite+CO_2 as a function of degree of partial melting at 15 and 30 kbar. *Am Mineral* **65**, 37–44 (1980).
147. Wyllie, P. J. & Huang, W. L. Carbonation and melting reactions in system CaO–MgO–SiO_2–CO_2 at mantle pressures with geophysical and petrological applications. *Contrib Mineral Petrol* **54**, 79–107 (1976).
148. Yaxley, G. M. & Brey, G. P. Phase relations of carbonate-bearing eclogite assemblages from 2.5 to 5.5 GPa: implications for petrogenesis of carbonatites. *Contrib Mineral Petrol* **146**, 606–619 (2004).
149. Minarik, W. G. & Watson, E. B. Interconnectivity of carbonate melt at low melt fraction. *Earth Planet Sci Lett* **133**, 423–437 (1995).
150. Helffrich, G. R. & Wood, B. J. The Earth's mantle. *Nature* **412**, 501 (2001).
151. Dasgupta, R., Hirschmann, M. M. & Smith, N. D. Partial melting experiments of peridotite + CO_2 at 3 GPa and genesis of alkalic ocean island basalts. *J Petrol* **48**, 2093–2124 (2007).
152. Mallik, A. & Dasgupta, R. Reactive infiltration of MORB-eclogite-derived carbonated silicate melt into fertile peridotite at 3 GPa and genesis of alkalic magmas. *J Petrol* **54**, 2267–2300 (2013).
153. Mallik, A. & Dasgupta, R. Effect of variable CO_2 on eclogite-derived andesite and lherzolite reaction at 3 GPa – implications for mantle source characteristics of alkalic ocean island basalts. *Geochem Geophys Geosyst* **15**, 1533–1557 (2014).
154. Guillot, B. & Sator, N. Carbon dioxide in silicate melts: a molecular dynamics simulation study. *Geochim Cosmochim Acta* **75**, 1829–1857 (2011).
155. Morizet, Y. et al. Towards the reconciliation of viscosity change and CO_2-induced polymerization in silicate melts. *Chem Geol* **458**, 38–47 (2017).
156. Langmuir, C., Klein, E. M. & Plank, T. Petrological systematics of mid-ocean ridge basalts: contraints on melt generation beneath ocean ridges. In: *Mantle Flow and Melt Generation at Mid-ocean Ridges, Geophysical Monograph Series* (eds. J. Phipps-Morgan, D. K. Blackman, & J. M. Sinton), 183–280 (American Geophysical Union, 1992).
157. Ghosh, S., Ohtani, E., Litasov, K. D. & Terasaki, H. Solidus of carbonated peridotite from 10 to 20 GPa and origin of magnesiocarbonatite melt in the Earth's deep mantle. *Chem Geol* **262**, 17–28 (2009).
158. Frost, D. J. et al. Experimental evidence for the existence of iron-rich metal in the Earth's lower mantle. *Nature* **428**, 409–412 (2004).
159. Rohrbach, A. et al. Metal saturation in the upper mantle. *Nature* **449**, 456–458 (2007).

160. Harmer, R. E. & Gittins, J. The origin of dolomitic carbonatites: field and experimental constraints. *J African Earth Sci* **25**, 5–28 (1997).
161. Nielsen, T. F. D., Solovova, I. P. & Veksler, I. V. Parental melts of melilitolite and origin of alkaline carbonatite: evidence from crystallised melt inclusions, Gardiner complex. *Contrib Mineral Petrol* **126**, 331–344 (1997).
162. Guzmics, T. et al. Primary carbonatite melt inclusions in apatite and in K-feldspar of clinopyroxene-rich mantle xenoliths hosted in lamprophyre dikes (Hungary). *Mineral Petrol* **94**, 225 (2008).
163. Woolley, A. R. & Church, A. A. Extrusive carbonatites: a brief review. *Lithos* **85**, 1–14 (2005).
164. Guzmics, T. et al. Carbonatite melt inclusions in coexisting magnetite, apatite and monticellite in Kerimasi calciocarbonatite, Tanzania: melt evolution and petrogenesis. *Contrib Mineral Petrol* **161**, 177–196 (2011).
165. Zaitsev, A. N. & Keller, J. Mineralogical and chemical transformation of Oldoinyo Lengai natrocarbonatites, Tanzania. *Lithos* **91**, 191–207 (2006).
166. Mitchell, R. H. Carbonatites and carbonatites and carbonatites. *Can Mineral* **43**, 2049–2068 (2005).
167. Weng, Z., Jowitt, S. M., Mudd, G. M. & Haque, N. A detailed assessment of global rare earth element resources: opportunities and challenges. *Econ Geol* **110**, 1925–1952 (2015).
168. Harmer, R. E. & Gittins, J. The case for primary, mantle-derived carbonatite magma. *J Petrol* **39**, 1895–1903 (1998).
169. Watkinson, D. H. & Wyllie, P. J. Experimental study of the composition join $NaAlSiO_4$–$CaCO_3$–H_2O and the genesis of alkalic rock–carbonatite complexes. *J Petrol* **12**, 357–378 (1971).
170. Neumann, E. R., Wulff-Pedersen, E., Pearson, N. J. & Spencer, E. A. Mantle xenoliths from Tenerife (Canary Islands): evidence for reactions between mantle peridotites and silicic carbonatite melts inducing Ca metasomatism. *J Petrol* **43**, 825–857 (2002).
171. Klein-BenDavid, O. et al. High-Mg carbonatitic microinclusions in some Yakutian diamonds – a new type of diamond-forming fluid. *Lithos* **112**, 648–659 (2009).
172. Kjarsgaard, B. & Peterson, T. Nephelinite–carbonatite liquid immiscibility at Shombole volcano, East Africa: petrographic and experimental evidence. *Miner Petrol* **43**, 293–314 (1991).
173. Guzmics, T., Zajacz, Z., Mitchell, R. H., Szabó, C. & Wälle, M. The role of liquid–liquid immiscibility and crystal fractionation in the genesis of carbonatite magmas: insights from Kerimasi melt inclusions. *Contrib Mineral Petrol* **169**, 17 (2015).
174. Weidendorfer, D., Schmidt, M. W. & Mattsson, H. B. Fractional crystallization of Si-undersaturated alkaline magmas leading to unmixing of carbonatites on Brava Island (Cape Verde) and a general model of carbonatite genesis in alkaline magma suites. *Contrib Mineral Petrol* **171**, 43 (2016).
175. Woolley, A. R. & Kjarsgaard, B. *Carbonatite Occurrences of the World: Map and Database* (Geological Survey of Canada, 2008).
176. Jelsma, H., Barnett, W., Richards, S. & Lister, G. Tectonic setting of kimberlites. *Lithos* **112**, 155–165 (2009).
177. Woolley, A. R. & Bailey, D. K. The crucial role of lithospheric structure in the generation and release of carbonatites: geological evidence. *Mineral Mag* **76**, 259–270 (2012).

178. Bell, K. & Tilton, G. R. Nd, Pb and Sr isotopic compositions of east African carbonatites: evidence for mantle mixing and plume inhomogeneity. *J Petrol* **42**, 1927–1945 (2001).
179. Bailey, D. K. Episodic alkaline igneous activity across Africa: implications for the causes of continental break-up. *Geol Soc Lond Spec Publ* **68**, 91–98 (1992).
180. Bell, K. Carbonatites: relationships to mantle-plume activity. *Geol Soc Am Special Paper*, **352**, 267–290 (2001).
181. Ernst, R. E. & Bell, K. Large igneous provinces (LIPSs) and carbonatites. *Mineral Petrol* **98**, 55–76 (2010).
182. Jelsma, H., Barnett, W., Richards, S. & Lister, G. Tectonic setting of kimberlites. *Lithos* **112**, 155–165 (2009).
183. Hoernle, K., Tilton, G., Le Bas, M. J., Duggen, S. & Garbe-Schonberg, D. Geochemistry of oceanic carbonatites compared with continental carbonatites: mantle recycling of oceanic crustal carbonate. *Contrib Mineral Petrol* **142**, 520–542 (2002).
184. Holm, P. M. et al. Sampling the cape verde mantle plume: evolution of melt compositions on Santo Antao, Cape Verde Islands. *J Petrol* **47**, 145–189 (2006).
185. Schmidt, M. W. & Weidendorfer, D. Carbonatites in oceanic hotspots. *Geology* **46**, 435–438 (2018).
186. Keshav, S. & Gudfinnsson, G. H. Experimentally dictated stability of carbonated oceanic crust to moderately great depths in the Earth: results from the solidus determination in the system CaO–MgO–Al_2O_3–SiO_2–CO_2. *J Geophys Res B Solid Earth* **115**, B05205 (2010).
187. Grassi, D. & Schmidt, M. W. The melting of carbonated pelites from 70 to 700 km depth. *J Petrol* **52**, 765–789 (2011).
188. Katsura, T., Yoneda, A., Yamazaki, D., Yoshino, T. & Ito, E. Adiabatic temperature profile in the mantle. *Phys Earth Planet Interiors* **183**, 212–218 (2010).
189. Hirschmann, M. M. Mantle solidus: experimental constraints and the effects of peridotite composition. *Geochem Geophys Geosyst* **24**, 1–26 (2000).
190. Gale, A., Dalton, C. A., Langmuir, C. H., Su, Y. & Schilling, J.-G. The mean composition of ocean ridge basalts. *Geochem Geophys Geosyst* **14**, 489–518 (2012).
191. Yasuda, A., Fujii, T. & Kurita, K. Melting relations of an anhydrous mid-ocean ridge basalt from 3 to 20 GPa: implications for the behviour of subducted oceanic crust in the mantle. *J Geophys Res* **99**, 9401–9414 (1994).
192. Wang, W. & Takahashi, E. Subsolidus and melting experiments of a K-rich basaltic composition to 27 GPa: implication for the behaviour of potassium in the mantle. *Am Mineral* **84**, 357–361 (1999).
193. Day, H. W. A revised diamond–graphite transition curve. *Am Mineral* **97**, 52–62 (2012).
194. Herzberg, C. & Gazel, E. Petrological evidence for secular cooling in mantle plumes. *Nature* **458**, 619 (2009).
195. Herzberg, C. et al. Temperatures in ambient mantle and plumes: constraints from basalts, picrites, and komatiites. *Geochem Geophys Geosyst* **8**, 2 (2007).